

891067

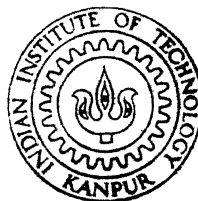
# SUPERPLASTICITY IN HIGH CARBON STEELS

By

R. K. JINDAL

ME  
1991  
M  
JIN  
3UP

Th  
me/1991/m  
J 5638



DEPARTMENT OF METALLURGICAL ENGINEERING  
INDIAN INSTITUTE OF TECHNOLOGY KANPUR  
MARCH, 1991

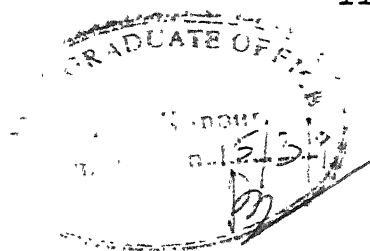
# SUPERPLASTICITY IN HIGH CARBON STEELS

*A Thesis Submitted*  
in Partial Fulfilment of the Requirements  
for the Degree of  
**MASTER OF TECHNOLOGY**

*By*  
R. K. JINDAL

*to the*  
DEPARTMENT OF METALLURGICAL ENGINEERING  
INDIAN INSTITUTE OF TECHNOLOGY KANPUR  
MARCH, 1991

ME-1991-M-DIN-SUP



## CERTIFICATE

This is to certify that the present investigation  
" SUPERPLASTICITY IN HIGH CARBON STEELS " has been carried  
out by Mr. R.K. Jindal under my supervision and that it has  
not been submitted elsewhere for a degree.

11111

(M.L. Vaidya)  
Professor  
Department of Metallurgical Engineering  
Indian Institute of Technology  
Kanpur



112198

Th  
669.142  
J 563 A

## ACKNOWLEDGEMENT

I owe my deep gratitude to Prof. M.L. Vaidya for his valuable guidance, supervision and persistent encouragement at every stage of this thesis work.

I also gratefully acknowledge the help provided by Prof. G.S. Murty and Prof. R.K. Dube.

My sincere thanks to staff members of laboratories/workshop especially Mr. H.C. Srivastava and Mr. B.K. Jain (A.C.M.S.) for providing help and excellent facility during the testing and equipment handling.

Thanks are also due to my friends, especially Manjusha, Lalitesh, Ravi, Atul and Satish for their valuable suggestions and immense inspiration, they gave throughout my work.

My sincere thanks are due to all the other who really worked for the preparation of this report. I wish to thank Mr. S. N. Pradhan for neat and patient typing.

R.K. Jindal

## CONTENTS

	Page
List of Tables	vii
List of Figures	viii
Abstract	x
CHAPTER I INTRODUCTION	1
1.1 Strain Rate Sensitivity Index	2
1.2 Factors Relating % Elongation in Tension Test	3
1.3 Cavitation Effect on Total Ductility	5
1.4 Necessary Conditions for Superplasticity	7
1.5 Production of Fine Grain Size	7
1.5.1 Grain Refinement by Phase Transfor- mation	9
1.5.2 Grain Refinement by Deformation of Duplex Alloys	9
1.5.3 Grain Refinement by Phase Separation	11
1.5.4 Grain Refinement by Recrystallization	12
1.5.5 Grain Coarsening Control	12
1.5.5.1 Grain Size Control by Particles	12
1.5.5.2 Grain Size Control by Partitioning	13
1.6 Applications of Superplasticity	13
1.6.1 Advantages of Superplasticity	14
1.6.2 Disadvantages of Superplasticity	14

	Page
CHAPTER II SUPERPLASTIC BEHAVIOUR IN IRON BASE ALLOYS	15
2.1 Commercial Applications	17
2.2 Objective of the Present Study	17
CHAPTER III EXPERIMENTAL PROCEDURE	20
3.1 Material Composition	20
3.2 Grain Refinement Treatments	20
3.2.1 Thermal Cycling	20
3.2.2 Single Quench Followed by Isoro-	
lling	21
3.3 Tensile Specimen Prepration	22
3.4 Mechanical Testing	25
3.4.1 Differential Strain Rate Test	25
3.4.2 Combination Test	26
3.5 Metallography and Fractrography	26
CHAPTER IV EXPERIMENTAL RESULTS	28
4.1 Microstructural Variation with Various	
Treatments	28
4.1.1 Microstructures of Thermally Cycled	28
Samples	
4.1.2 Microstructures of Single Quench-	
Isorolled Samples	31
4.1.3 Microstructures of Samples After	
Mechanical Testing	31
4.1.4 General Remarks on Microstructures	35
4.2 Stress-Strain Rate Behaviour	35
4.3 Strain Rate Sensitivity Index-True Strain	38

4.4 Effect of Repeated Strain Rate Cycling on True Stress - True Strain Rate Behaviour	38
4.5 % Elongation-Strain Rate Sensitivity Index Relationship	42
CHAPTER V DISCUSSIONS	44
5.1 Microstructures	44
5.2 Stress-Strain Rate Behaviour	46
5.3 Strain Rate Sensitivity Index-Strain Rate Behaviour	46
5.4 % Elongation-Strain Rate Sensitivity Index	47
5.5 Superplasticity in High Carbon Steels.	47
CHAPTER VI CONCLUSIONS	50
REFERENCES	51
APPENDIX	

## List of Tables

Page

Table- 1	Various treatments given to samples in summary.	23
----------	----------------------------------------------------	----

## List of Figures

Page

Fig. 1.1	Graphical Representation of Equation (1.3) Dependence of Rate of Decrease of area on cross sectional area for different values of 'm'.	4
Fig. 1.2	General mechanisms of grain refinement.	10
Fig. 2.1	The Iron-Carbon phase diagram.	19
Fig. 3.1	Tensile sample (Flat).	34
Fig. 4.1	Microstructure of as received high carbon steel, Sample-1.	29
Fig. 4.2a	Microstructure of thermally cycled Sample-3, (940°C/OQ/ 5 cycles/650°C)	29
Fig. 4.2b	Microstructure of Sample-3 at higher magnification.	29
Fig. 4.3	Microstructure of thermally cycled Sample-4, (940°C/OQ/10 cycles/650°C).	29
Fig. 4.4	Microstructure of thermally cycled Sample-6, (900°C/OQ/10 cycles /650°C).	30
Fig. 4.5	Microstructure of Sample-7, (850°C/WQ/2 cycles/650°C).	30
Fig. 4.6a	Microstructure of thermally cycled Sample-8, (900°C-880°C/OQ/5 cycles/560°C).	30
Fig. 4.6b	Microstructure of Sample-8, at higher magnification.	30
Fig. 4.7a	Microstructure of quenched-isorolled Sample-9, (900°C/OQ/55% reduction).	32
Fig. 4.7b	Microstructure of Sample -9, at higher magnification.	32
Fig. 4.8	Microstructure of Sample-10, (850°C/OQ/75% reduction).	32
Fig. 4.9	Microstructure of Sample-11 (880°C/OQ/79% reduction).	32
Fig. 4.10	Microstructure of Sample-12, (820°C/OQ/80% reduction).	33

Fig. 4.11	Fracture surface of Sample-5.	33
Fig. 4.12	Fracture surface of Sample- 9.	33
Fig. 4.13a	Microstructure of Sample-3, before mechanical testing.	34
Fig. 4.13b	Microstructure of Sample-3 after mechanical testing.	34
Fig. 4.14a	Microstructure of Sample-10, before mechanical testing.	34
Fig. 4.14b	Microstructure of Sample-10, after mechanical testing.	34
Fig. 4.15	True stress vs, true strain rate plots for different thermally cycled samples.	36
Fig. 4.16	True stress vs true strain rate plots for different quenched-isorolled samples.	37
Fig. 4.17	Strain rate sensitivity index vs true strain rate plots for different thermally cycled samples.	39
Fig. 4.18	Strain rate sensitivity index vs true strain rate plots for different quenched-isorolled samples.	40
Fig. 4.19	Effect of repeated cycling on stress-strain rate behaviour for different samples.	41
Fig. 4.20	Relation between % elongation and 'm'.	43
Fig. 5.1	Comparison between the standard and present relationship between % elongation and 'm'.	48



## ABSTRACT

High carbon steel containing 1.0% carbon steel has been subjected to thermal cycling and quench-isorolling techniques to get fine structure. The austenitization temperature, quenching medium and number of cycles were varied to optimise the conditions for best structure by thermal cycling. In case of single quench-isorolling, the austenitization temperature and % reduction in rolling were varied. Samples obtained from the above techniques were tested at 700°C in tension using differential strain rate tests and constant speeds to evaluate their ductility and stress-strain rate behaviour. Variance of % elongation with strain rate sensitivity index has also been noted.

It has been concluded that superplasticity can be induced in this type of steel by single quench-isorolling technique. Quenching in oil from 880°C followed by isorolling at 720°C to total % reduction of 79% gives best results of ductility. However in thermal cycling, quenching in water from 850°C, repeatedly cycling for two cycles, followed by annealing at 650°C for 30 minutes, gives good values of % elongation. Ductilities exceeding 300% have been obtained in the given steel by quench-isorolling technique.

## CHAPTER - I

### INTRODUCTION

Most metals and alloys exhibit elongations to failure of less than 50% when pulled in tension at elevated temperatures. Super plastic alloys are capable of exhibiting very large elongations to failure, typically greater than 300%.

Superplasticity is defined as the ability of a material to exhibit large tensile elongations and is associated with high strain rate sensitivity. The large tensile elongations and typically low flow stresses associated with superplastic metals and alloys permit the forming of complex and intricate shapes by using methods forming pressures not previously possible.

Superplasticity in metals and alloys has attracted the attention of scientists and technologists over a considerable number of years. There has been great deal of work devoted to both the fundamental and technological aspects of superplasticity. Alloys of considerable commercial interest have been developed and there are number of practical forming operations currently in use which utilise superplastic deformation. In recent years, the subject has been reviewed in part in technical journals and an impressive number of research papers have been published.

Superplastic alloys usually exhibit a sigmoidal relationship between the flow stress and the strain rate, on a logarithmic scale, and these data may be divided conveniently into three regions, each of which is represented frequently in the form

$$\sigma = K\dot{\epsilon}^m \quad \dots (1.1)$$

where  $\sigma$  is the flow stress,  $K$  is a constant,  $\dot{\epsilon}$  is the strain rate and ' $m$ ' is the strain rate sensitivity index. Superplastic elongations to failure are intermediate strain rates in region-II where the value of  $m$  is typically greater than 0.4. The elongations to failure decrease at lower strain rates in region I and at higher strain rates in region III, where the respective values of ' $m$ ' are typically less than 0.3.

### 1.1 Strain Rate Sensitivity Index:

Strain rate sensitivity index is a very important parameter in characterising superplastic deformation. From the equation 1.1

$$m = \frac{d(\ln \sigma_t)}{d(\ln \dot{\epsilon}_t)} \quad \dots (1.2)$$

This is the slope of the  $\ln \sigma_t - \ln \dot{\epsilon}_t$  curve.

There are various methods of measuring ' $m$ ' but broadly all lead to a variation of ' $m$ ' with  $\dot{\epsilon}_t$ . ' $m$ ' also varies with temperature and structure. The value ' $m$ ' increases with decreasing grain size and / or increasing temperature.

The temperature dependence of 'm' is more in region II compared with either region I or III. In case where the 'm' value is independent of strain rate it is found to increase monotonically with temperature.

Strain rate sensitivity index 'm' has a maximum value at a critical strain rate,  $\dot{\epsilon}_t^*$ , which in general, increases with increasing temperature but there has been cases where it is independent of temperature.

## 1.2 Factors Relating % Elongation in Tension Test:

Testing at high temperature and low strain rates accentuates superplastic behaviour. It is clear that large elongations result from the suppression of necking in these materials with high value of strain rate sensitivity index, 'm'. (1)

In normal metal the geometric softening that constitutes the formation of neck is opposed by strain hardening and so long as  $d\sigma/d\epsilon > \sigma$ , the tensile specimen will not neck down. With a superplastic material the rate of strain hardening is low (because of high temperature or structural condition) but necking is prevented by the presence of strain rate hardening, and  $d\sigma/d\epsilon > \sigma$ . The following equation has been drawn

$$-\frac{dA}{dt} = \left(\frac{P}{C}\right)^{1/m} \left(\frac{1}{A^{(1-m)/m}}\right) \dots (1.3)$$

Graphical representation of equation 1.3 has been shown in Fig. 1.1. Equation 1.3 states that so long as 'm' is  $\ll 1$ , the smaller the cross sectional area, the more rapidly area is reduced. Fig 1.1 shows how the area decrease varies with 'm'. When  $m=1$ , the deformation is newtonian viscous

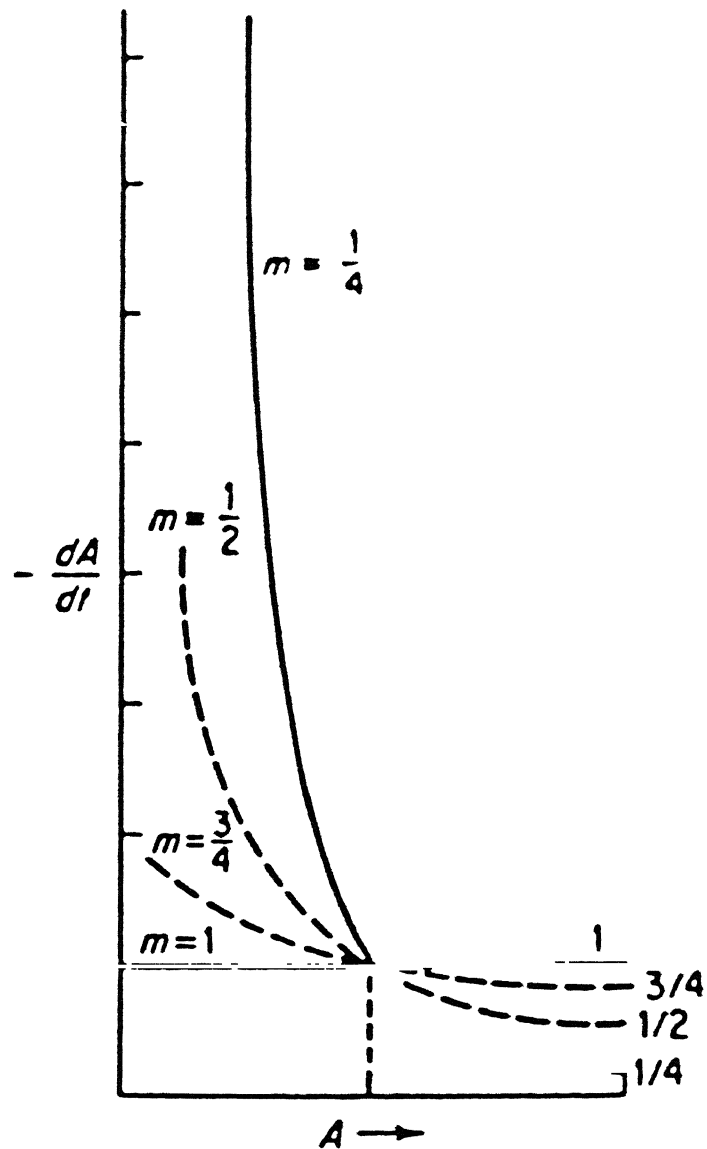


Fig. 1.1 Graphical representation of Equation(1.3). Dependence of rate of decrease of area on cross-sectional area for different values of 'm'.

and  $dA/dt$  is independent of  $A$  and any incipient neck is simply prevented during elongation and does not propagate inward. As ' $m$ ' approaches unity the rate of growth of incipient neck is drastically reduced.

In general, a direct relation between the value of ' $m$ ' and the elongation exists. But none of the analytical or empirical equations presented predicts superplastic elongations satisfactorily, though the following equations are comparatively more accurate.<sup>(2)</sup>

$$\% \text{ elongation} = e_0 + 100 [(1 - \alpha^{1/m})^{-m} - 1] \quad \dots (1.4)$$

$$\% \text{ elongation} = Bm^2(d_0/l_0)100 \quad \dots (1.5)$$

Where  $e_0$  is the elongation for  $m=0$ ,  $B$  is a constant  $d_0$  is the initial specimen diameter and  $l_0$  is the original gauge length.

Moreover, the elongation of strip specimens is inferior to that of round one. Elongation to fracture increases with decreasing grain size but often it goes through a maximum with strain rate. Also there is some evidence that the elongation to fracture in microduplex alloys is maximum when the ratio of the phases is approximately unity<sup>(3)</sup>.

### 1.3 Cavitation Effect on Total Ductility:

At elevated testing temperatures, failure in tension may occur by two processes: (a) external necking and (b) internal cavitation. In general, superplastic alloys do not exhibit much

external necking when tested under optimal conditions.

Cavitation plays an important role in the failure of superplastic alloys to such an extent that in some alloys excessive cavitation may lead to premature failure. Cavitation failure involves the nucleation, growth and interlinkage of cavities<sup>(4)</sup>.

Cavities nucleate continuously during superplastic deformation. Microstructural inspection of superplastically deformed alloys, reveals, the alignment of cavities in stringers parallel to the tensile axis. A possible explanation for this observation is that large agglomerated particles are broken up along the extrusion or rolling direction and cavities are subsequently nucleated at these sites.

In general, cavity growth may occur by the stress directed diffusion of vacancies into cavities or by the plastic deformation of the material surrounding a cavity. In fine grained superplastic alloys, cavities are observed frequently with dimensions substantially larger than the grain size. Under these conditions, cavity growth may occur also by a superplastic deformation mechanism, in which vacancy diffusion into cavities occur along the many grain boundaries intersected by large cavities<sup>(5)</sup>.

Several different techniques have been developed to reduce cavitation damage during superplasticity, these include (a) annealing superplastically formed components at elevated temperature (b) hot isostatically pressing superplastically formed components and (c) superimposition of

hydrostatic pressures during superplastic forming.

#### 1.4 Necessary Conditions for Superplasticity:

The existence of fine grained ( $<10\ \mu\text{m}$ ) equiaxed polyphase structures, with the phases displaying similar ductility at the temperature of deformation, is conducive to superplasticity. The rates of deformation should be such as to give 'm' values of 0.3 or more. The temperature of deformation should be greater than  $0.4\ T_m$ , where  $T_m$  is the absolute melting temperature. Duplex and multiphase structures have stable grain sizes which are resistant to grain growth and these alloys are significantly more superplastic. The type of phase or phases, their distribution, the grain boundary condition, temperature, strain rate and grain size all influence the degree of superplasticity. In iron-carbon alloys undissolved carbides, residual massive martensite and non-equilibrium structures have been shown to prevent superplasticity.

Cast or cast and homogenised alloys of eutectic, eutectoid or polyphase compositions are also not superplastic although in the wrought condition they exhibited significant superplasticity. The difference has been attributed variously to the lamellar, dendritic or interlocking nature of grain boundaries in the cast alloys. <sup>(6)</sup>

#### 1.5 Production of Fine Grain Size:

One of the simplest methods for producing an fine grain size is to cast alloys of eutectic, eutectoid or



polyphase compositions and subsequent working them by about 60 to 80 percent to obtain an intimate mixture of phases. Evidently in this case stable fine grains of less than 10  $\mu\text{m}$  size can be obtained even when the particles are relatively coarse and well separated. This method has been extensively employed to induce superplastic behaviour in a number of systems e.g. Pb-Cd eutectic, Zn-Al eutectoid, Al-Cu eutectic, etc. Moreover alloys of Copper, Nickel as well as some alloy steels contain a high volume fraction of the second phase and therefore can be processed by the above procedure. In these cases however, often a thermo-mechanical treatment becomes necessary.

However, as the temperature of the superplastic deformation are usually of the order of  $0.5 T_m$  or more, considerable coarsening of the particles is likely. Thus only fine particles that coarsen very slowly should be employed. In case of low carbon as well as low alloy steels, by adding appropriate combination of  $\alpha$  and  $\gamma$  stabilisers and hot working the alloy, stable, duplex structures that give rise to superplastic properties at optimal temperatures could be generated, e.g. Aluminium addition to low carbon steels.

The powder metallurgy route has advantage particularly when compositional variation can cause difficulties. For instance, in conventionally formed nickel base superalloys segregation and banding are severe problems.

Solid reactions such as spinoidal decomposition or rapid heating to a two phase field have been successfully employed to produce random, fine grain structures. In alloy

steels, controlled thermal cycling leads to a fine grained microstructure<sup>(7)</sup>. Schematic diagram is shown in Fig. 1.2<sup>(8)</sup>.

#### 1.5.1 Grain Refinement by Phase Transformation:

In this case the aim is to nucleate several product grains within each grain of the parent microstructure. The ferrite-austenite phase transformation has been used for grain refinement in steels. Several studies have shown that cycling repeatedly through the transformation temperature results in very fine grain sizes. The mechanism of grain refinement in this case is nucleation of the product phase at grain boundaries in the parent phase. As grain size becomes finer during successive cycles, more nucleation sites are available for the next transformation. Eventually, at submicrometer grain sizes, the grain size saturates and further cycling does not produce additional grain refinement.

In recent years, the controlled rolling has been developed to produce fine grain sizes in High-strength Low Alloy steels. Controlled rolling can be done as a continuous process, unlike thermal cycling; thus, controlled rolling is more suitable for large scale production. The key to grain refinement by controlled rolling is transformation to ferrite of hot-worked, uncrystallized austenite. The heavily deformed austenite provides a high density of nucleation sites for ferrite grains and the transformed ferrite grain is extremely fine.

#### 1.5.2 Grain Refinement by Deformation at Duplex Alloys:

Grain refinement of duplex alloys that already have a duplex equilibrium microstructure is accomplished by

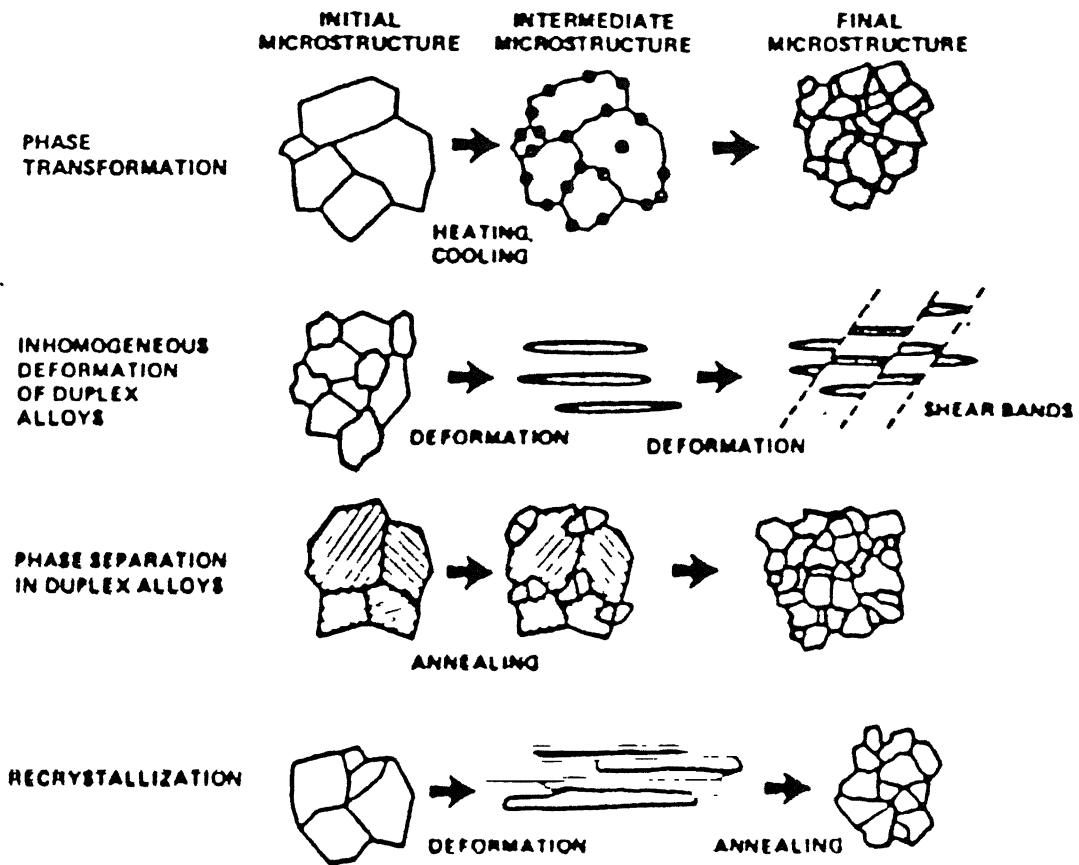


Fig. 1.2 General mechanisms of grain refinement.

extensive deformation ( rolling or extrusion are commonly used) near the temperature range where superplasticity is observed. Annealing treatment is frequently used after deformation, although dynamic recrystallization generally occurs during deformation. However, recrystallization alone cannot produce a finer, intermixed, two phase microstructures. Homogeneous deformation of a duplex structure will produce elongated phase regions, perhaps recrystallized so that each original grain contains several recrystallized grains, but the phases will not intermixed. Elongated phase regions are indeed broken up during deformation. Annealing permits recrystallization of each phase and allows sufficient diffusion for spheroidization to the desired equiaxed fine grain structure.

### 1.5.3 Grain Refinement of Phase Separation in Duplex Alloys:

Annealing duplex alloys with a non-equilibrium microstructure causes phase separation into the two equilibrium phases. Separation of the initial microstructure into the two equilibrium phases ( $\alpha$  and  $\beta$ ) can produce a fine grain duplex microstructure.<sup>(9)</sup> The non equilibrium starting microstructure is usually martensite or a quenched solid solution. The substructure present in martensite microstructures frequently provide a high density of nucleation sites for the equilibrium phases. Warm deformation of quenched solid solutions prior to phase separation can be used to enhance grain refinement during phase separation. Grain refinement of duplex alloys by phase separation has been used in Titanium alloys and Zn-Al alloys.

#### 1.5.4 Grain Refinement by Recrystallization:

Recrystallization is a universal technique for grain refinement. In recent years, recrystallization has been extensively studied in aluminium base alloys, also an excellent understanding of the effects of particles on a recrystallization has been developed.

Two modes of recrystallization can be used for grain refinement, both rely on particles to produce fine grain size. The well known discontinuous recrystallization mode occurs by nucleation and growth of recrystallized grains. In this case, a key factor in grain refinement is formation of a high density of nucleation sites for recrystallizing grains. Continuous recrystallization is the alternate recrystallization mode available for grain refinement.

#### 1.5.5. Grain Coarsening Control:

In addition to starting with a fine grain size, grain growth must be suppressed during the slow superplastic forming process at elevated temperature. Two general methods available for grain size control are : the pinning force exerted on boundaries by solute atoms and particles, and the alloying element partitioning that occurs in duplex alloys.

##### 1.5.5.1 Grain Size Control by Particles:

Particles restrict grain growth by exerting a drag force on migrating boundaries. The origin of the drag force is the reduction of grain boundary energy that occurs when the boundary intersects the particle. Based on the drag force

exerted on a grain boundary by a particle dispersion, one can calculate the grain size at which grain growth is arrested. All classes of superplastic alloys except duplex alloys employ particle for grain size control.

#### 1.5.5.2 Grain Size Control by Partitioning

In duplex alloys, grain growth is restricted by partitioning of alloying elements between the two phases. After grain refinement many  $\alpha$ - $\alpha$  and  $\beta$ - $\beta$  grain boundaries are present, along with the  $\alpha$ - $\beta$  boundaries. Grain coarsening occurs initially by elimination of many  $\alpha$ - $\alpha$  and  $\beta$ - $\beta$  boundaries, leaving unconnected grains of each phase. For further grain growth, diffusion is required.

### 1.6 Applications of Superplasticity:

The characteristic features of deformation of alloys which exhibit superplasticity is that extremely high strains can be achieved with low applied stresses with a high strain-rate sensitivity during deformation. The high strain rate sensitivity makes these alloys resistant to localised deformation (necking or thinning). Additionally it is recognised that conventional compressive working processes, e.g. rolling and forging, could benefit from the low flow stresses associated with superplastic deformation. Then smaller working loads and lower stresses on tooling would result. There are, however, possible disadvantages. The most significant of these is the requirement to work within a limited and relatively low, strain rate range. It is also necessary to establish a combination of microstructural and deformation

conditions which avoids premature rupture during forming, in particular internal cavitation must not occur.

There are number of forming operations used with superplastic alloys, which include hydraulic buldging, sheet thermoforming, blow moulding, deep drawing, punch stretching, forging and stamping, extrusion, dieless drawing etc.

#### 1.6.1 Advantages of Superplastic Forming:

Vastly improved formability is obtained compared with conventional forming processes even for high strength low ductility materials. Thus processes requiring large amounts of deformation can be performed in one operation, often producing components with complex shape. As a result multistage manufacturing processes that involve extensive welding or machining may be bypassed, or previously unattainable shapes may be produced<sup>(10)</sup>.

Forming pressures are drastically reduced; in some cases enough to make feasible the use of cheaper, novel, or more lightweight, forming equipment.

Considerable cost savings may be made. Also wastage is minimized. A uniform microstructure is produced which leads to uniform reproducible, mechanical properties throughout the body of the finished product.

#### 1.6.2 Disadvantages of Superplastic Forming:

The creep properties of the component are often inferior to those obtained by conventional forming routes, primarily because of the fine grain size. The process is not suitable for rapid mass production techniques although reasonably short forming times are possible.

## CHAPTER II

### SUPERPLASTIC BEHAVIOUR IN IRON BASE ALLOYS

Iron base alloys are probably the most versatile and in many contexts, the most important of all structural materials. It is not surprising, therefore, that work carried out soon after the revival of interest in superplasticity in the western world in the first half of the 1960's included attempts to develop microstructural superplasticity in steels.

However it has been observed that, plain carbon steels of hypoeutectoid and eutectoid composition cannot be heat treated to make them capable of sustaining superplastic flow to any significant extent. This is because the steels do not contain a sufficiently large volume fraction of cementite (12% at 0.8% carbon) to prevent rapid growth of ferrite grains at the superplastic deformation temperatures<sup>(11)</sup>.

In an attempt to circumvent these problems, steels containing carbon between 1.2-2.1% were examined. It was reasoned that the increased volume of  $\text{Fe}_3\text{C}$  would reduce ferrite grain growth without increasing brittleness, since  $\text{Fe}_3\text{C}$  had been shown to exhibit high plasticity at temperatures near the  $A_1$ .<sup>(12)</sup> The other advantage of these steels is that above  $A_1$  temperature austenite grain growth should be inhibited by the presence of  $\text{Fe}_3\text{C}$ .

A variety of thermal and thermomechanical treatments have been developed to obtain a matrix of very fine ferrite grains. (0.5-1.5  $\mu\text{m}$ ), containing very small particles of spheroidised  $\text{Fe}_3\text{C}$ . A typical grain refining treatment involves



homogenisation in the austenite range to take all the carbon into solution, followed by rolling during cooling through the  $\gamma + \text{Fe}_3\text{C}$  range to just below  $A_1$  temperature.

Also it has been noted that high purity high carbon steels can not be made superplastic and show lower values of 'm'. The addition of Chromium has been found to increase superplastic elongations of the order of 1500%. Apart from the work on Chromium, the effect of a range of dilute alloying additions on the microstructure of high carbon steels after processing, and on superplastic behaviour have been examined.

Apart from the thermomechanically procedure it has been demonstrated that heat treatment alone can refine the as cast microstructure of a high carbon steel. The heat treatment which involves oil-quenching from  $1150^\circ\text{C}$  followed by repeated cycling across the  $A_1$  temperature, lead to a markedly refined structure although as fine as that produced by thermo-mechanical processing. With an optimum structure, elongation to failure of the order of 300% have been achieved. By the method of single quenching followed by isorolling of high carbon steels, quite good percentage of elongation have been achieved<sup>(13)</sup>.

Fine structures generally lead to good room temperature properties such as strength, ductility and toughness. The case of high carbon steels is no exception. In the wrought, non-heat treated condition, high strengths combined with good ductilities have been obtained.

The carbon content of high carbon steels has the inherent advantage that extremely high hardness ( $R_c=65-68$ ) can be achieved upon appropriate heat treatment. Further, the unique fineness of the structure of high carbon steel is retained after transformation and leads to an unusual property compression ductilities of upto 10% in a material having a compression fracture strength of about 650 ksi<sup>(14)</sup>.

Same study has been done on duplex stainless steel also. They have an advantage that they are superplastic, at temperatures of 900-1000°C, after normal processing and do not require any further treatment.

## 2.1 Commercial Applications:

Interest in the superplastic forming of steel has up to the early 1980's been relatively limited despite the observation behaviour in a wide range of alloys. However there is a commercial interest in the microduplex stainless steels and development work on the forming of various complex shapes from sheet material has been carried out. A further area of commercial interest is in the superplastic hobbing of die steels. Required structure can be produced in various die steels by quenching and tempering, and have applications of superplastic hobbing.

## 2.2 Objective of The Present Study:

Traditionally, steels containing 1.0 to 2.1% carbon, have been neglected by industry in modern times. The discoveries made have revealed, however that such steels

demand a thorough assessment as they have the potential to emerge important technological materials. The steels, when processed to develop ultra-fine ferrite grains, 0.5-2.0  $\mu\text{m}$ , containing fine spheroidized particles, have been shown to be superplastic. Fig. 2.1 shows the Fe-C phase diagram.

Previous studies have indicated that there are varieties of way, superplastic structure can be induced in a conventionally produced high carbon steels namely; thermo-mechanical treatments, thermal cycling etc. But no systematic comparison has been made regarding their effects. Further, even in methodology adopted, the processing variables have not been studied.

In the present study, an attempt has been made to study effects of two methods of obtaining fine grained structure viz., thermal cycling and quenching followed by isothermal rolling, on the total elongation that can be obtained in high carbon steel containing 1.0% carbon. The other purpose of the study is to find whether superplastic behaviour can be induced in ultra-high carbon steel containing high % of chromium ( used as cold-working die material) by a simple technique of thermal cycling.

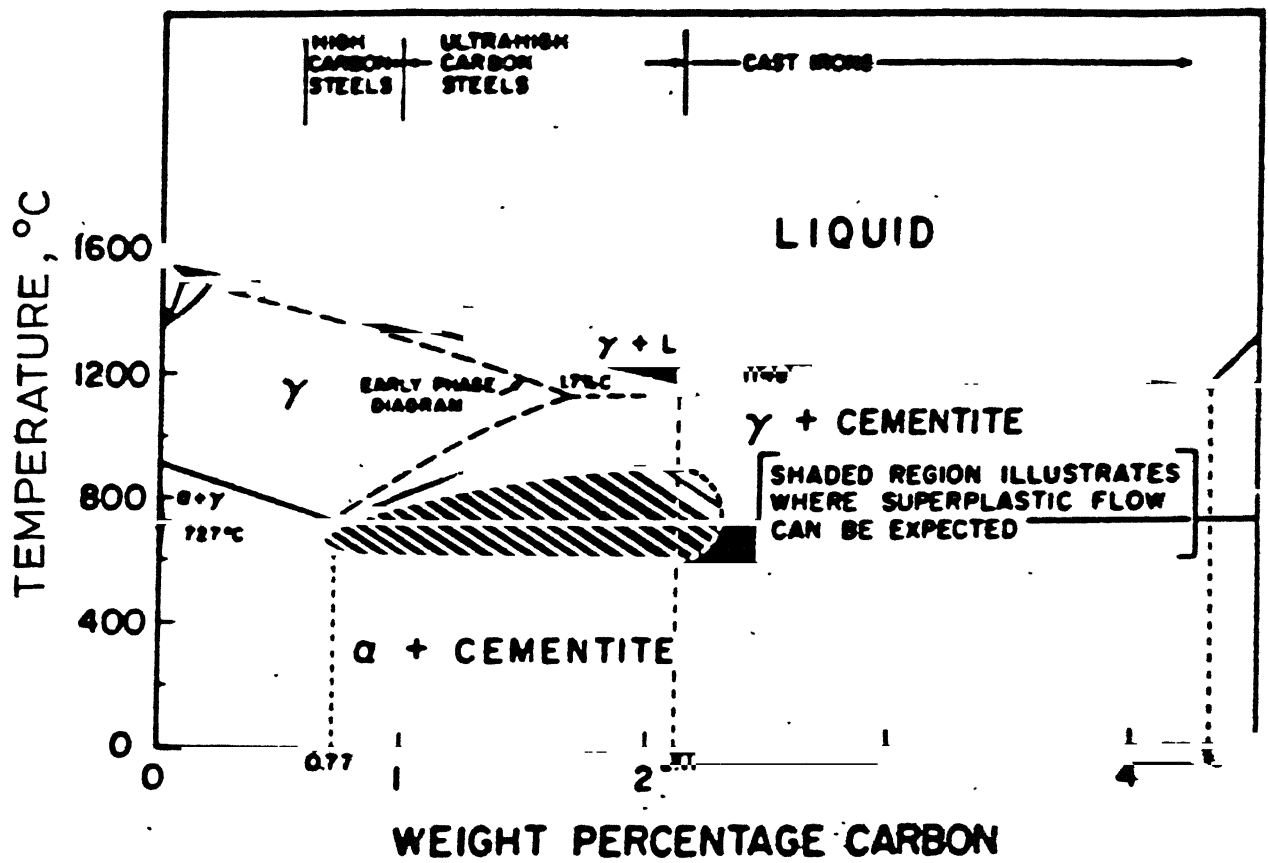


Fig. 2.1 THE IRON-CARBON PHASE DIAGRAM

## CHAPTER III

### EXPERIMENTAL PROCEDURE

#### 3.1 Material Composition:

Two types of steels were used for the present study.

- (i) Plain high carbon steel having carbon content 1.0%
- (ii) High carbon high chromium steel of 2.0% carbon and 12% chromium. These types of steels are generally air hardening steels.

#### 3.2 Grain Refinement Treatments:

The following two methods were adopted for the grain refinement of the steels.

##### 3.2.1 Thermal Cycling:

It is the process in which the material is heated to austenitization temperature and then rapidly cooled. Then this process is repeated for number of cycles. In present work the different combination of austenitization temperature and number of cycles were used to optimise the condition for grain refinement and cementite spheroids distribution.

- (a) The sample was heated to austenitization temperature  $940^{\circ}\text{C}$  and then quenched in water. This process of heating and cooling around the transformation temperature was carried out for five cycles. The cracks were observed in the specimen. However the sample was annealed at  $650^{\circ}\text{C}$  for 30 minutes.

(b) To avoid the cracking the quenching medium was changed to oil and the same above process was carried out for five cycles, and ten cycles.

(c) However it was felt that the austenitization temperature could be decreased. Sample was heated to  $900^{\circ}\text{C}$  and then quenched in oil. The same method was performed for 10 cycles. Then annealed at  $650^{\circ}\text{C}$  for 30 minutes.

(d) Sample was heated to  $900^{\circ}\text{C}$  and then quenched in oil. In next heating, the austenitization temperature was decreased by  $5^{\circ}\text{C}$  from  $895^{\circ}\text{C}$ . Total four cycles were given. Then annealed at  $650^{\circ}\text{C}$  for 30 minutes.

(e) It was observed that the austenitization temperature could be further lowered by quenching in water. Sample was heated to  $850^{\circ}\text{C}$  and quenched in water. Then the sample was heated to  $840^{\circ}\text{C}$  and quenched, annealed at  $650^{\circ}\text{C}$  for 30 minutes.

(f) The high carbon high chromium steel was heated to  $900^{\circ}\text{C}$  and quenched in oil. While heating again the austenitization temperature was decreased by  $5^{\circ}\text{C}$ . Total 5 cycles were given. Then the sample was annealed at  $650^{\circ}\text{C}$  for 30 minutes.

### 3.2.2 Single Quench Followed by Isorolling:

The samples were quenched from the austenitization temperature and then rolled at a constant temperature. Rolling at constant temperature is attained by heating the samples after each pass.

(a) Sample with initial thickness of 10 mm was heated to  $900^{\circ}\text{C}$ , quenched in oil and isorolled at  $720^{\circ}\text{C}$ . Total reduction was 55% in six passes.

(b) Sample with initial thickness 11 mm was heated to 850°C, quenched in oil, and isorolled at 740°C to total reduction of 75% getting final thickness of 2.7 mm. 10 passes with different reduction were given.

(c) Sample was heated to 880°C, quenched in oil, and isorolled at 720°C to total reduction of 79%.

(d) Sample was heated to 820°C, quenched in oil, and isorolled at 720°C to total reduction of 80%. 12 passes with different reductions were given.

Table-1 shows the various treatments in summary of all the samples.

### 3.3 Tensile Specimens Prepration:

All the samples received after all the above stated processes, were machined to get the tensile specimen of the shape shown in Fig.3.1. The specimens were cut on band saw and then to remove any scale formed these were machined on shaper. In the case of single quench isorolled samples, these were cut along the rolling direction. To precisely get the required dimensions, these were machined at surface grinder in precision shop.

Before the actual test the specimens were annealed to relieve any stresses introduced during machining of the specimens. Annealing after the machining also helps in reducing cavitation effect on the total ductility of the specimen.

TABLE - 1

SAMPLE NO.	TREATMENT
1.	As received condition
2.	940°C/WQ/5 cycles/ 650°C
3.	940°C/OQ/5 cycles/650°C
4.	940°C/OQ/10 cycles/650°C
5.	900°C/OQ/10 cycles/650°C
6.	900-885°C/OQ/4 cycles/650°C
7.	850-840°C/WQ/2 cycles/650°C
8.	900-880°C/OQ/5 cycles/650°C
9.	900°C/OQ/ 55% reduction
10.	850°C/OQ/75% reduction
11.	880°C/OQ/ 79% reduction
12.	820°C/OQ/ 80% reduction



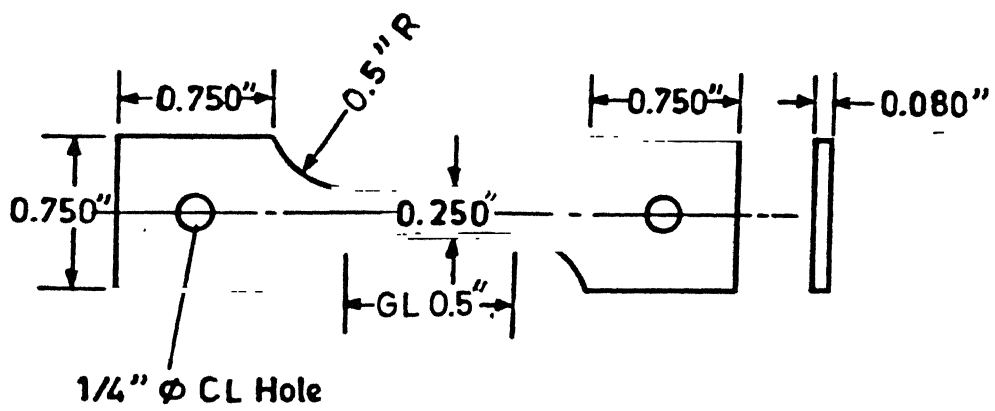


Fig. 3.1 Tensile sample (Flat)

### 3.4 Mechanical Testing:

All the specimens were tested on Instron Universal Testing Machine 1195. This machine has the capability of changing the crosshead speed as well as chart speed during the deformation of the specimen. The furnace attached was heated to the required temperature. There were three different zones of heating in the furnace. However the proper combination of current was chosen for three zones such that the heated zone only remains over the tensile specimen without heating grips very much. The sample was loaded into the furnace 15 minutes before the actual test so that it gets uniform temperature before test. The temperature of the sample was controlled by the furnace and monitored throughout the test by the additional Alumel-Chromel thermocouple fitted in the middle of the sample. Tensile tests were carried out at a constant temperature of  $700^{\circ}\text{C}$  controlled by a three zone heating coil furnace with an accuracy of  $\pm 02.0^{\circ}\text{C}$ .

True stress, true strain rate, were calculated from the load-time record during the deformation. All the calculations for the instant area of cross-section, true stress, true strain rate etc., were done in computer and the Fortran-77 programme and results are shown in Appendix.

#### 3.4.1 Differential Strain Rate Test:

To get the value of strain rate sensitivity index 'm', differential strain rate tests were carried out starting with the initial crosshead speed of 0.05 mm/min,

the speed was successively increased to next higher level upto the maximum speed of 2.0 mm/min. The load corresponding to each of the crosshead speed was thus recorded.

The strain rate sensitivity index 'm' was calculated by the relation

$$m = \frac{\ln (P_2/P_1)}{\ln (V_2/V_1)}$$

Where  $P_1$  and  $P_2$  are the steady state loads corresponding to crosshead speeds  $V_1$  and  $V_2$  respectively.

### 3.4.2 Combination Test:

Few samples were used for differential strain rate test in combination with constant cross head speed. At some instances the differential strain rate test was carried out to check for the steady state.

In the begining of the test, the differential strain rate tests were carried out to find the crosshead speed or rather strain rate giving highest value of 'm'. And further tests was carried out at that crosshead speed till rupture.

### 3.5 Metallography and Fractrography:

All samples were cut to proper shape for metallography. The usual polishing procedure starting from belt grinder to series of emery papers and cloth polishing by Alumina powder, were adopted. The etchant for revealing the ferrite boundaries to differentiate from carbides,

5 ml nitric acid, with 4 grams of picric acid dissolved in methyl alcohol to make 100 ml, was used. The other etchant was 3% nital. The specimens were etched for 10 to 15 seconds. As the grain size was very fine so it was not quite clear to observe the distribution of cementite spheroids, so scanning electron microscope was used.

The same procedure was used for the mechanically tested specimens, after cutting them near the rupture. Fracture surface was also observed on the scanning electron microscope. To remove any dust, the surface was simply washed by methanol.

## CHAPTER IV

### EXPERIMENTAL RESULTS

The results of the various experiments performed according to the procedures explained in the previous chapter are presented below. The order in which the results are shown is:

- (1) Microstructures obtained by various thermal cycling and single quench-isorolling techniques.
- (2) Stress vs strain rate data for different samples.
- (3) Strain rate sensitivity index vs strain rate for different samples.
- (4) Effect of repeated strain rate cycling on true stress-true strain rate behaviour.
- (5) % elongation vs strain rate sensitivity index 'm'.

#### 4.1 Microstructure Variation with Various Treatments:

Fig. 4.1 shows microstructure of as received material (1.0% carbon steel ) and it is observed that grain size is quite large of the order of 20  $\mu\text{m}$ . The structure is lamellar in nature.

##### 4.1.1 Microstructures of Thermally Cycled Samples:

Fig. 4.2 to Fig. 4.6 show microstructures of various thermally cycled samples. It has been observed that size of the cementite spheroids is of the order of 2  $\mu\text{m}$  in case of oil quenched sample. Interlinkage between the cementite spheroids is quite clear. However in case of water

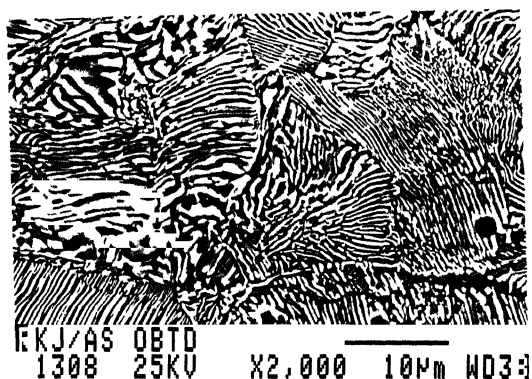


Fig. 4.1 Microstructure of as received high carbon steel, Sample-1.

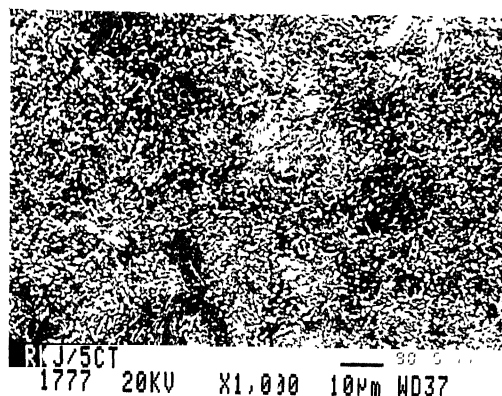


Fig. 4.2a Microstructure of thermally cycled Sample -3.  
( 940°C/OQ/5cycles/650°C)

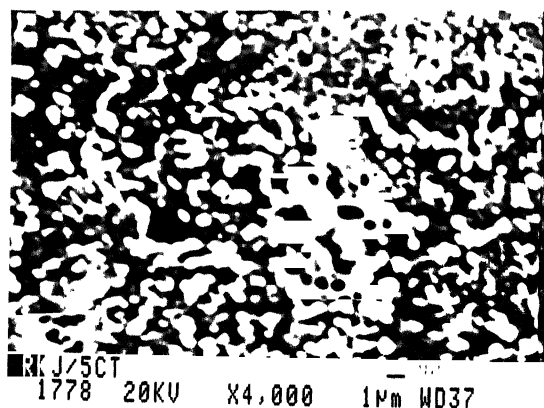


Fig. 4.2b Microstructure of Sample-3 at higher magnification.

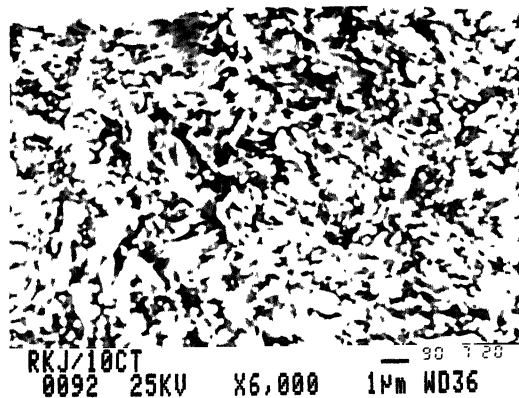


Fig.4.3 Microstructure of thermally cycled Sample-4  
(940°C/OQ/10 cycles/650°C)

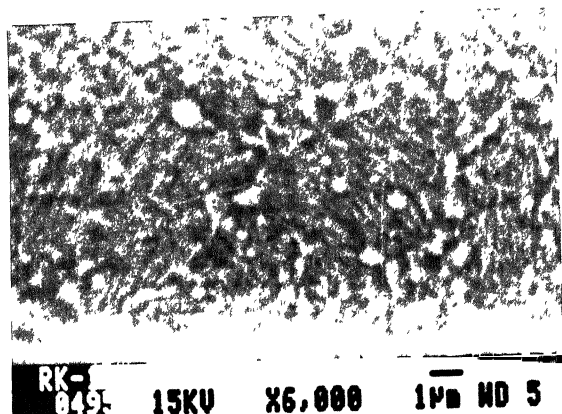


Fig.4.4 Microstructure of thermally cycled Sample-6 (900°C/OQ/10 cycles/650°C)

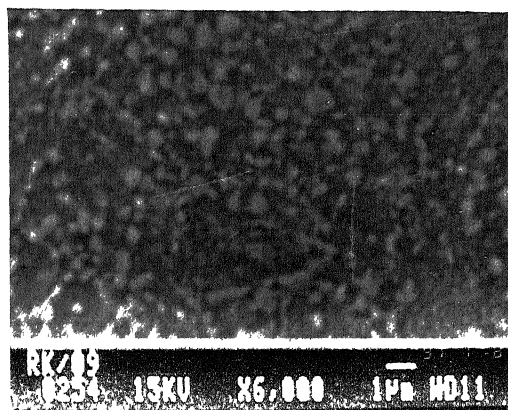


Fig. 4.5 Microstructure of Sample -7 (850°C/WQ/2 cycles/650°C)

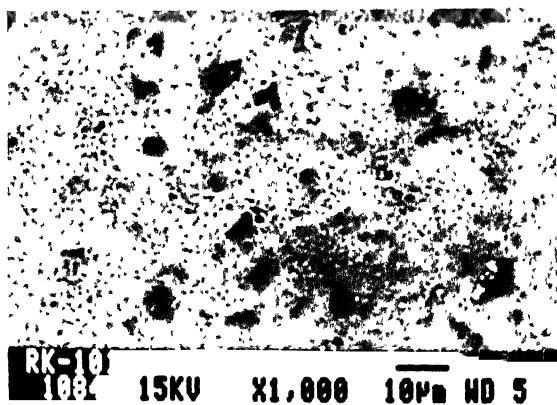


Fig.4.6a Microstructure of thermally cycled Sample-8 (900°C-880°C/OQ/5 cycles/650°C)

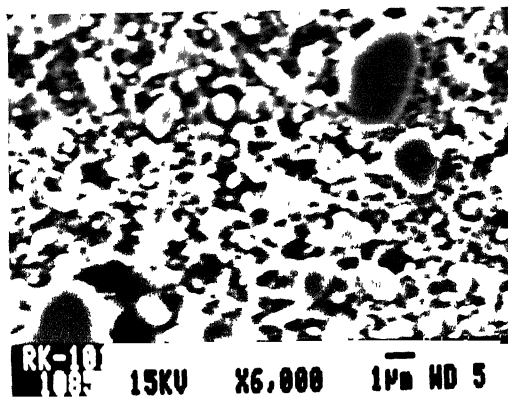


Fig. 4.6b Microstructure of Sample -8 at higher magnification.

quenched samples, the structure is more fine and size of spheroids is of the order of  $1\text{ }\mu\text{m}$ . Also there is good distribution of spheroids in the ferrite matrix. Comparing five cycled and ten cycled samples, it has been observed that increasing number of cycles gives no further refinement, but coarsens the structure.

#### 4.1.2 Microstructures of Single Quenched-Isorolled Samples:

Fig. 4.7 to Fig. 4.10 show microstructures of various quenched-isorolled samples. In all the cases it has been observed that the structure is more fine as compared to thermally cycled samples. It is also noted that % reduction in rolling and austenitization temperature has a considerable effect on the final structure. By increasing % reduction, the structure has been made more and more fine. However temperature of austenitization should be such that it dissolves all the carbon before it is subjected to rapid cooling i.e. quenching.

#### 4.1.3 Microstructures of Samples After Mechanical Testing:

Fig. 4.11 and Fig. 4.12 show the fractured surface of various samples. It is observed that the fracture is ductile with some exception at few places where cavities are observed.

Fig. 4.13 and Fig. 4.14 compare the microstructures of various samples, before mechanical testing with those of after mechanical testing. It is observed that in



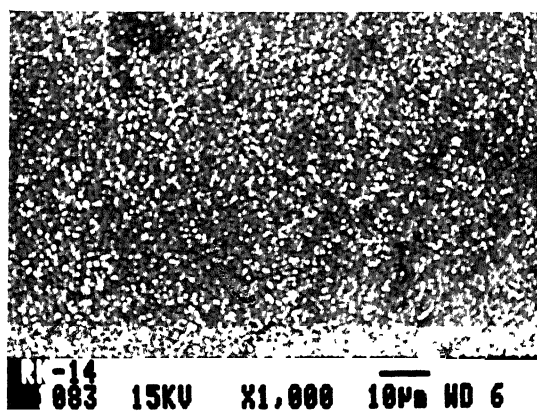


Fig. 4.7a Microstructure of quenched-isorolled Sample-9 ( $900^{\circ}\text{C}/\text{OQ}/55\%$  reduction).

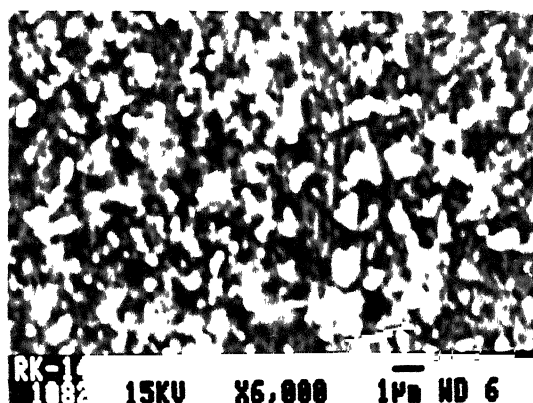


Fig.4.7b Microstructure of Sample -9 at higher magnification.

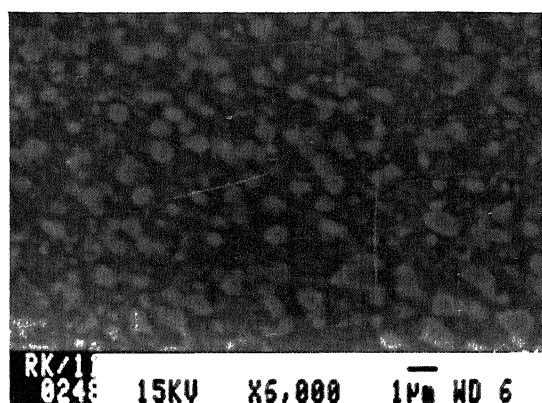


Fig. 4.8 Microstructure of Sample -10 ( $850^{\circ}\text{C}/\text{OQ}/75\%$  reduction)

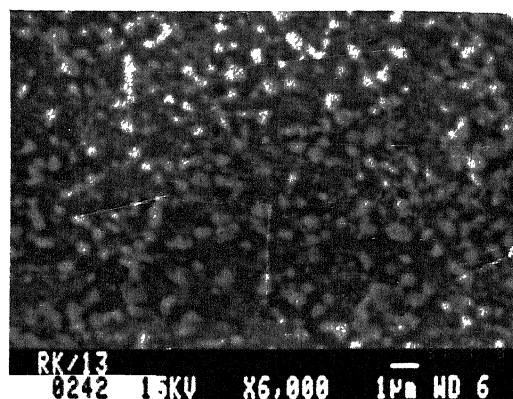


Fig.4.9 Microstructure of Sample-11 ( $880^{\circ}\text{C}/\text{OQ}/79\%$  reduction)

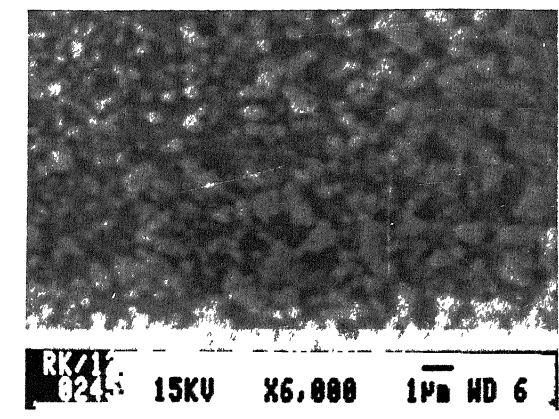


Fig. 4.10 Microstructure of  
Sample- 12-  
(820°C/0Q/80% reduction.

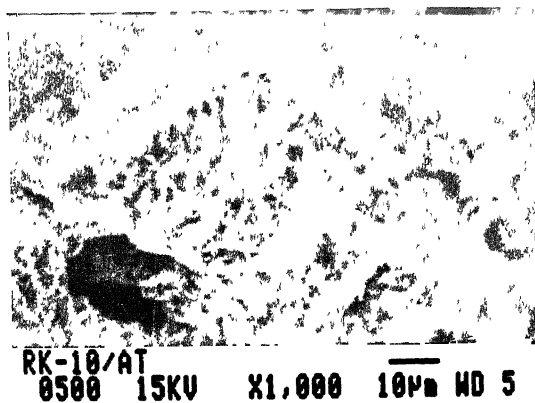


Fig. 4.11 Fracture surface of  
Sample -5

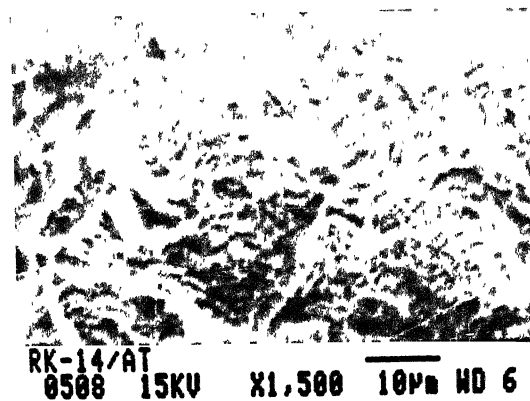


Fig. 4.12 Fracture surface of  
Sample -9

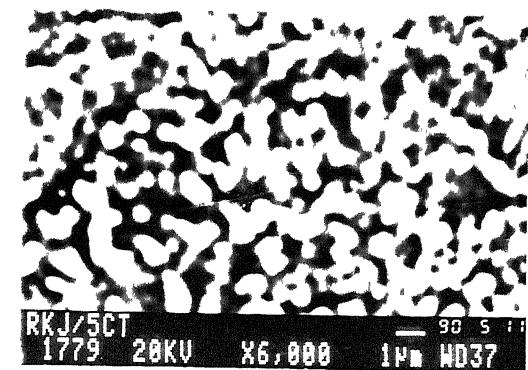


Fig. 4.13a Microstructure of Sample-3 before mechanical testing.

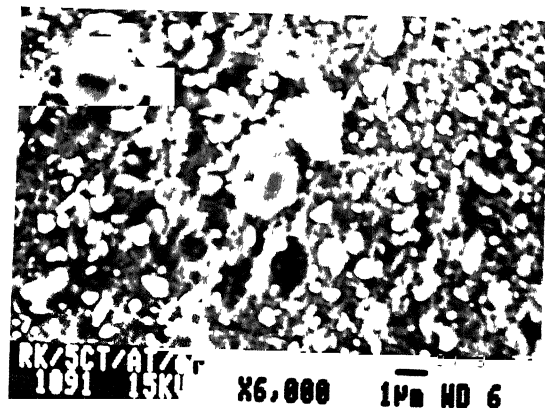


Fig. 4.13b Microstructure of Sample-3 after mechanical testing.

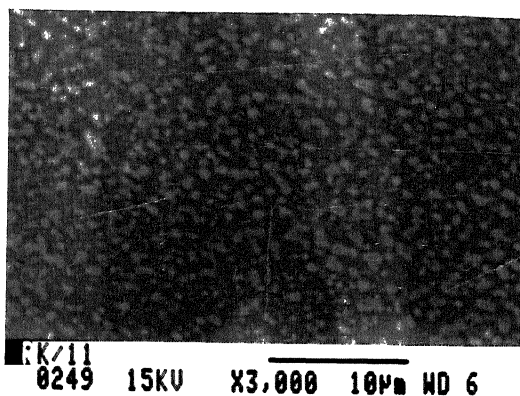


Fig. 4.14a Microstructure of Sample-10 before mechanical testing .

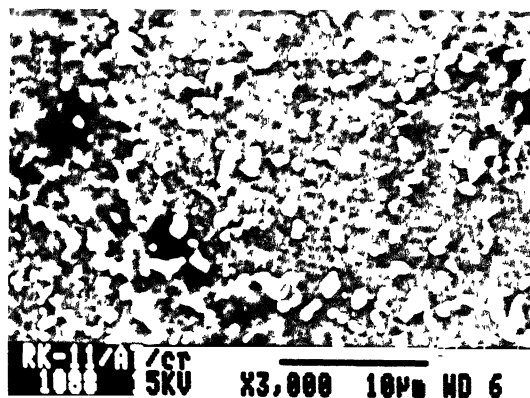


Fig.4.14b Microstructure of Sample -10 after mechanical testing.

case of thermally cycled samples, considerable coarsening has taken place. At few places cavities are quite clear. While in case of quenched-isorolled sample, the coarsening is comparatively less.

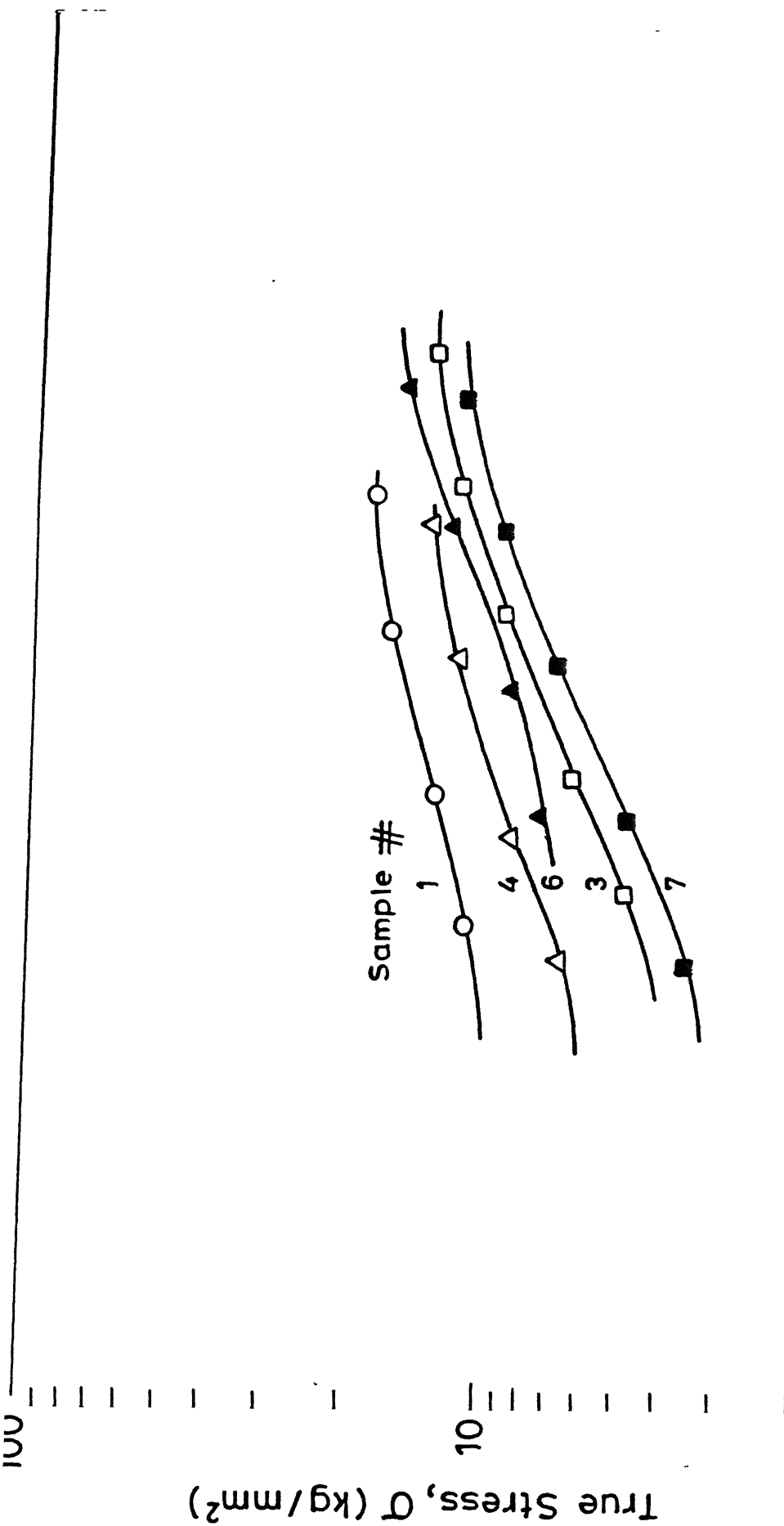
#### 4.1.4 General Remarks on Microstructures:

It is observed that increasing number of cycles does not help in refining the structure. The austenitization temperature can be lowered to  $850^{\circ}\text{C}$  by changing the quenching medium from oil to water, which gives good fineness and distribution of cementite spheroids, but the structure is not as fine as that of quenched-isorolled samples. It is also noted that the extent of coarsening during the deformation is less in case of quenched-isorolled samples as compared to thermally cycled samples.

#### 4.2 Stress-Strain Rate Behaviour:

The stress-strain rate data have been plotted and shown in Fig. 4.15 and Fig. 4.16, for various samples. The data have been presented on log-log graph. The data for sample in as received condition have also been plotted to compare with the data for thermally cycled samples. As far as the true stress levels are concerned, each sample shows a different level. Sample in as received condition shows the highest level of true stress at a given strain rate. It is followed by the samples processed by thermal cycling.

In Fig. 4.16, the curves show the data for different samples in quenched-isorolled condition. The



Refer to Table -1 for sample details

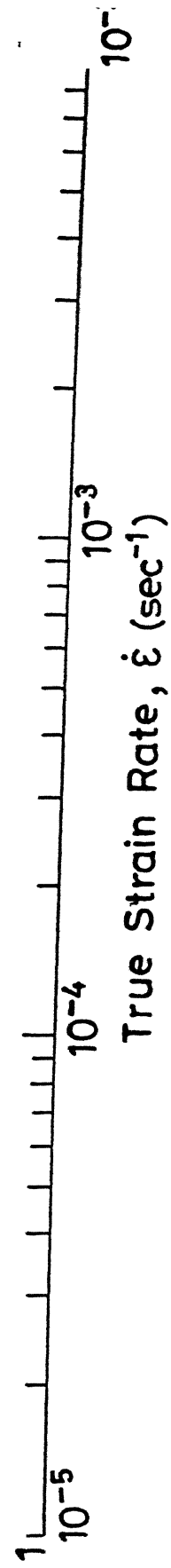


Fig.4.15 True stress vs.true strain rate plots for different thermally cycled samples.

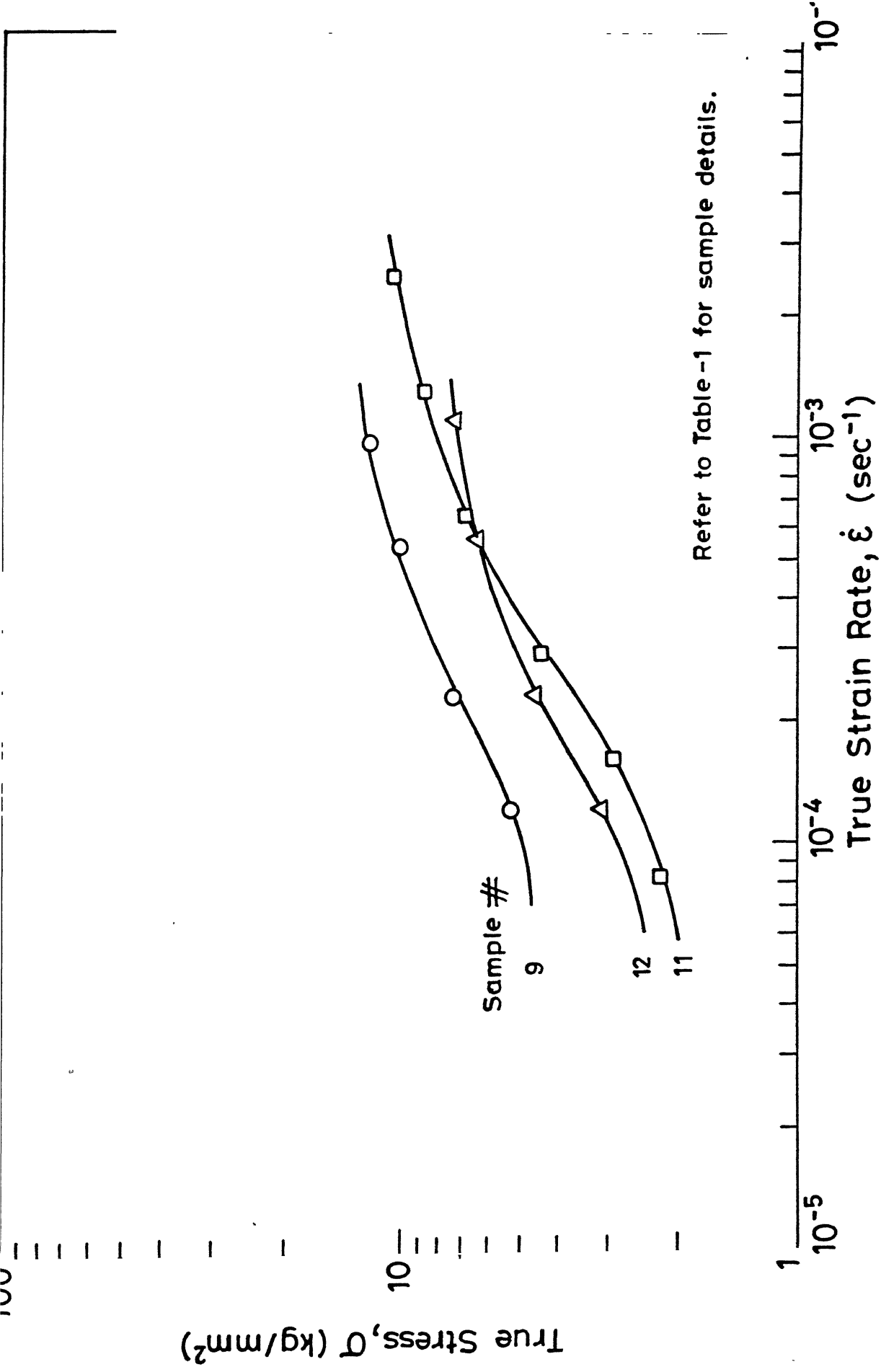


Fig.4.16 True stress vs true strain rate plots for different quenched-isorolled samples.

nature of the curve is sigmoidal i.e. the slope changes from a low value at low strain rates to higher value at the intermediate strain rates and again decreases to a lower value at high strain rates. The levels of true stress are still in the lower side as compared to the as received and thermally cycled samples.

#### 4.3 Strain Rate Sensitivity Index-True Strain Rate Behaviour:

The data of strain rate sensitivity index, ' $m$ ', and true strain rate have been presented on semi-log graphs. Fig. 4.17 shows the plots of ' $m$ ' versus  $\dot{\epsilon}$  for thermally cycled samples. In all cases, ' $m$ ' is low at lower and higher strain rates and exhibit a maximum at intermediate strain rates. The same features are noted for quenched-isorolled samples, whose data are presented in Fig. 4.18. The peak ' $m$ ' values occur at different strain rate levels and the maximum value of ' $m$ ' differs from treatment to treatment.

In case of quenched-isorolled samples highest value of ' $m$ ' of the order of 0.476 has been achieved while in case of thermally cycled samples, the maximum value of ' $m$ ' is around .33 only. Also the percentage elongation achieved is more in the case of quenched-isorolled samples followed by the thermally cycled samples.

#### 4.4 Effect of Repeated Strain Rate Cycling on True Stress-True Strain Rate Behaviour:

Fig. 4.19 shows the effect of repeated cycling on stress- strain rate behaviour for sample-7 and sample-8

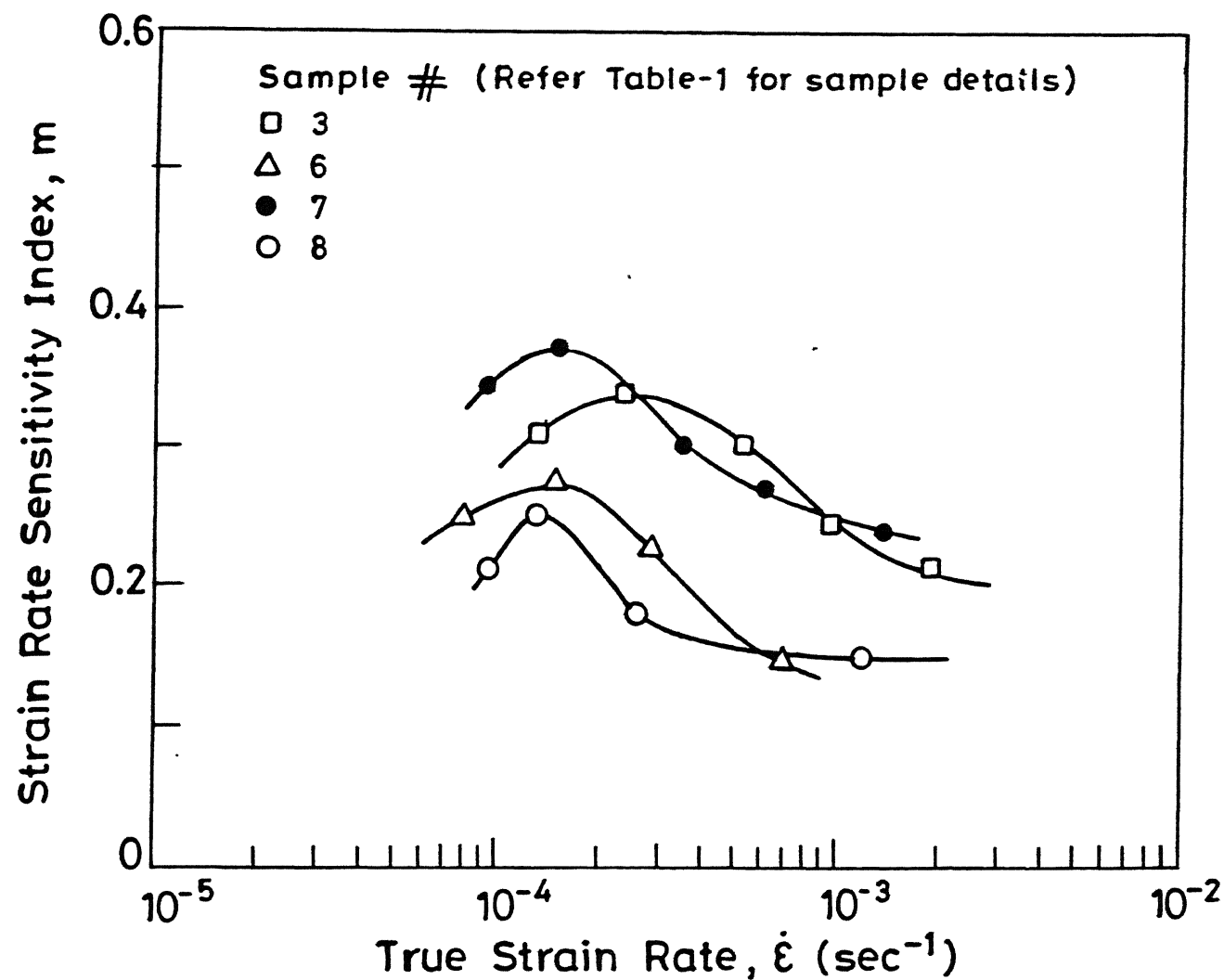


Fig.4.17 Strain rate sensitivity index vs.true strain rate plots for different thermally cycled samples.



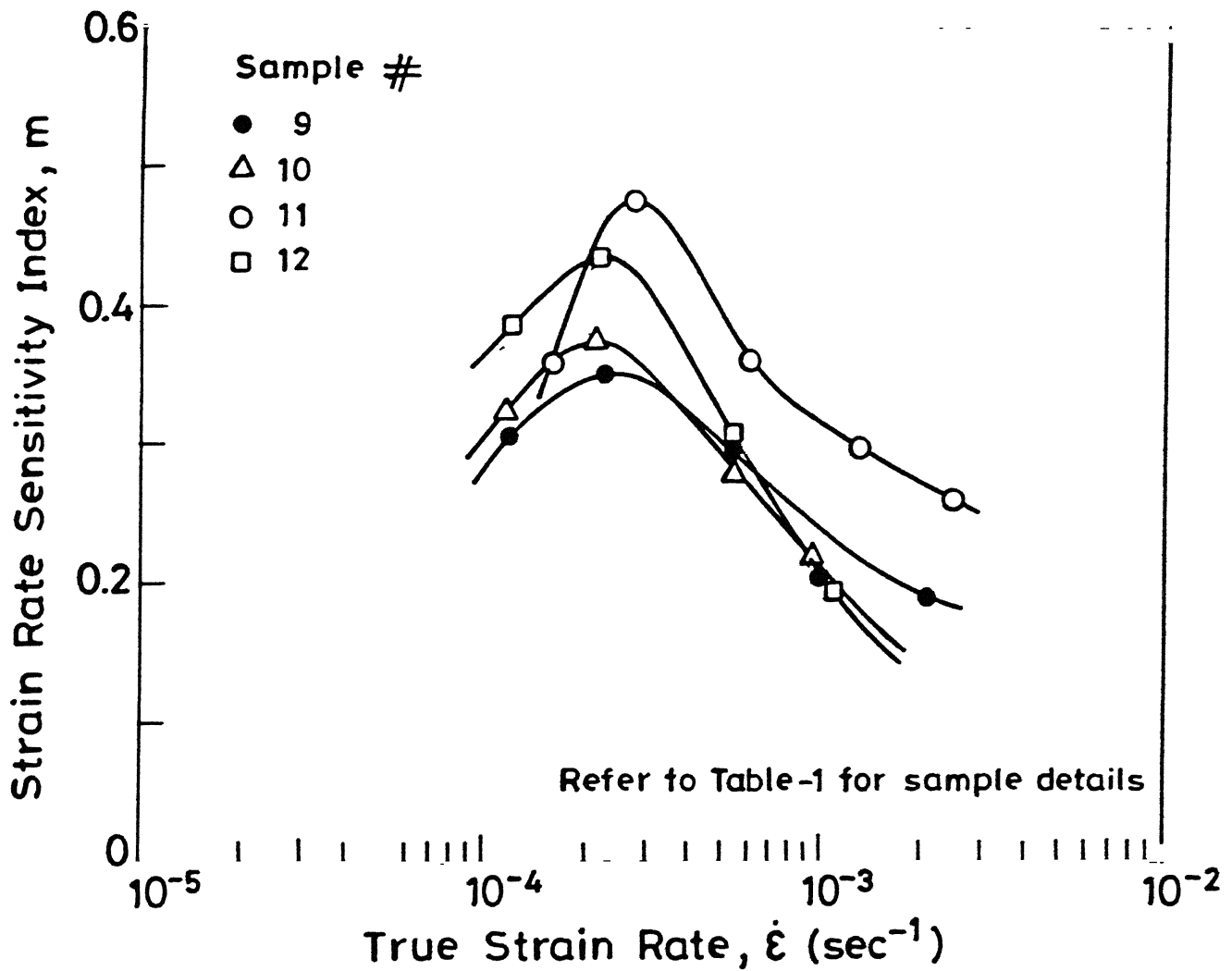


Fig.4.18 Strain rate sensitivity index vs. true strain rate plots for different quenched - isorolled samples.

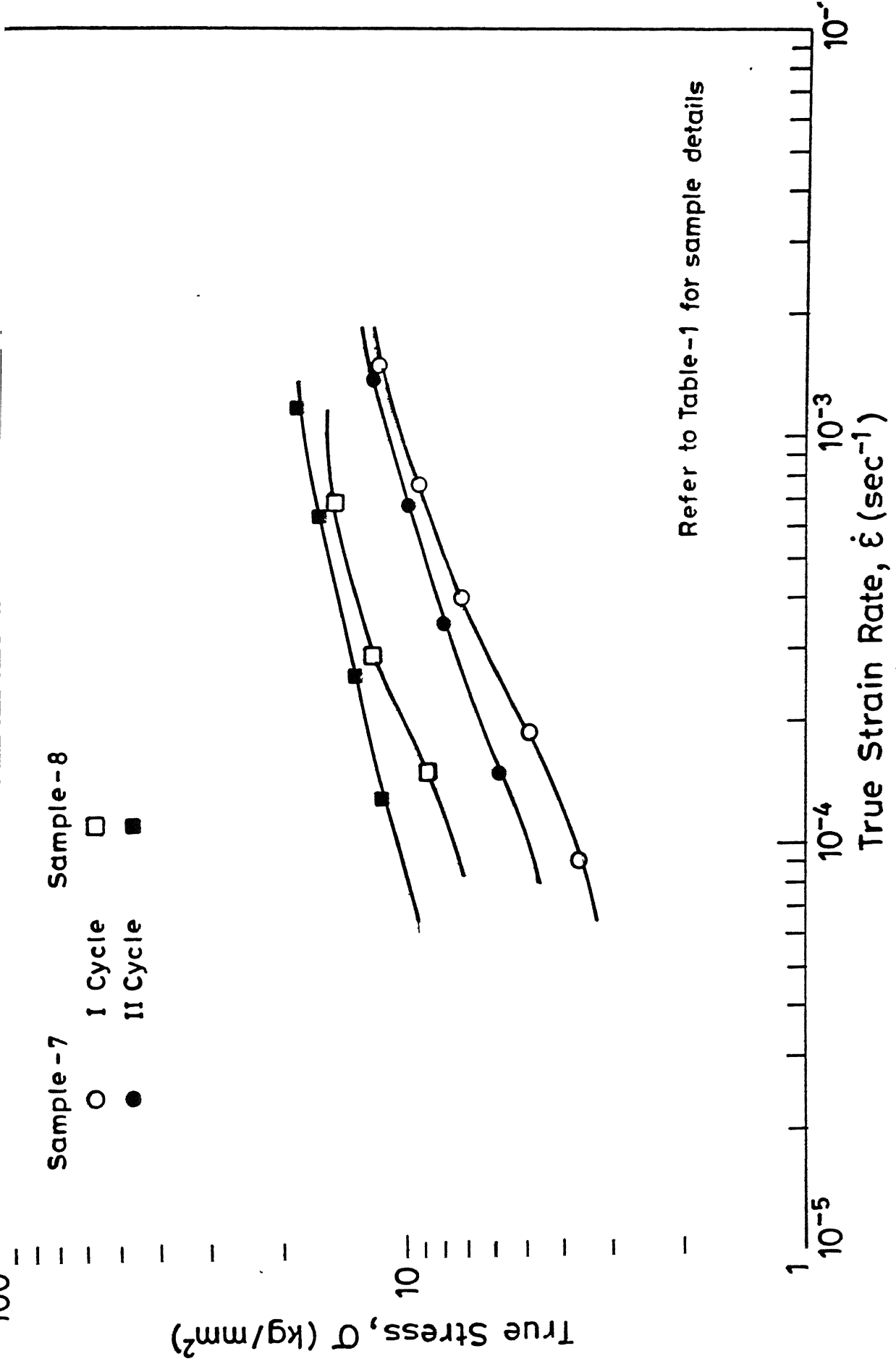


Fig.4.19 Effect of repeated cycling on stress-strain rate behaviour for different samples.

Change in flow stress is very less at higher strain rates though at the lower strain rates, considerable change in flow stress is observed.

#### 4.5 % Elongation- Strain Rate Sensitivity Index Relationship:

Fig. 4.20 shows the plot of % elongation to rupture vs strain rate sensitivity index 'm' of different samples. From the figure it is clear that as the value of 'm' increases, % elongation also increases. In case of thermally cycled samples the value of 'm' does not exceed 0.38, so accordingly % elongation also does not exceed 200%. In case of single quenched-isorolled sample, the value of 'm' reaches to 0.476, so large elongations have been achieved.

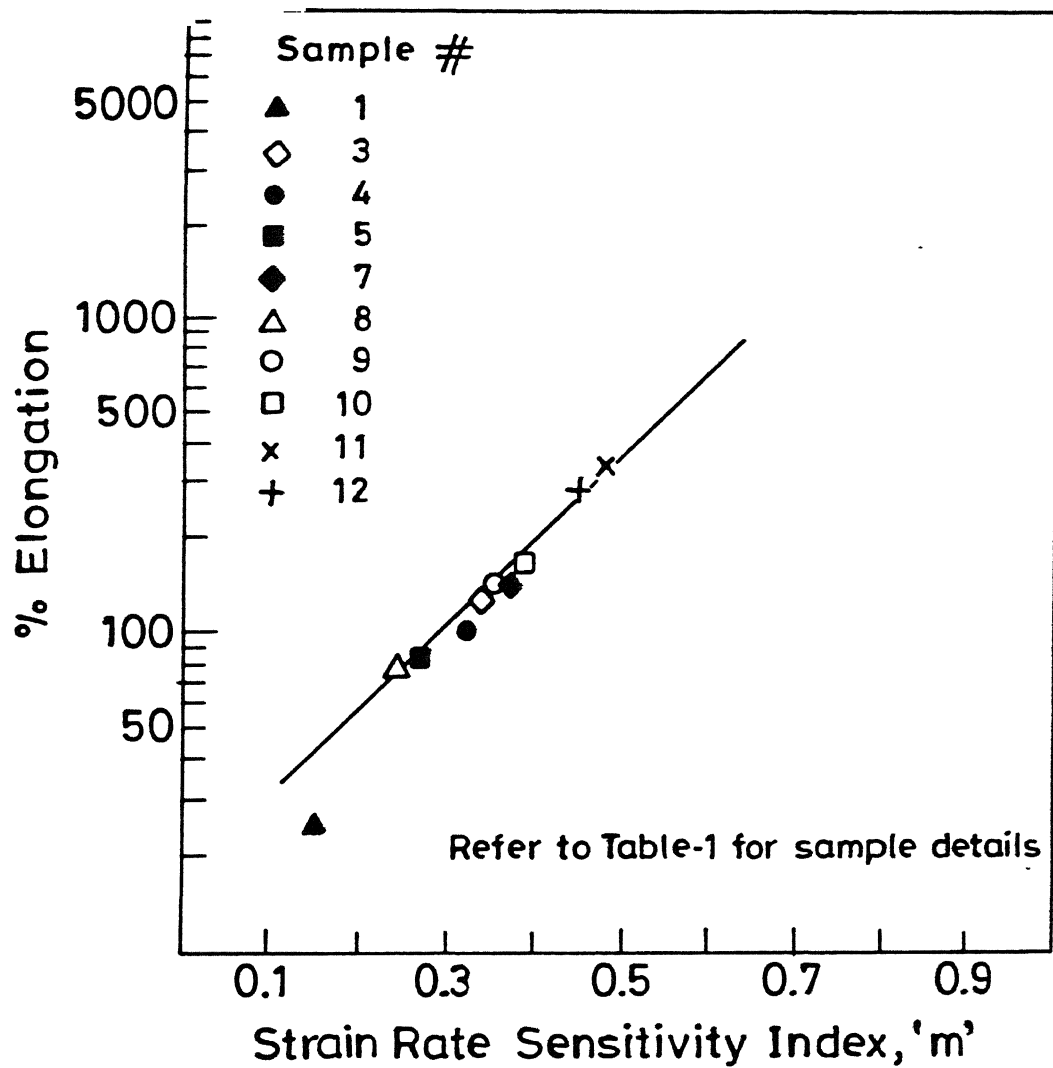


Fig.4.20 Relation between % elongation and 'm'.

## CHAPTER V

### DISCUSSIONS

All the results including microstructures, various plots such as (a) Stress-strain rate (b) Strain rate sensitivity index- true strain rate (c) Effect of repeated cycling on true stress-true strain rate behaviour and (d) % elongation- strain rate sensitivity index, shown in the previous Chapter IV are explained here.

#### 5.1 Microstructures:

The material in its as received condition shows the microstructure of pearlite with some grain boundary cementite which shows that carbon content of steel is more than 0.8%.

After thermal cycling, fine structure with cementite spheroids has been achieved. In Sample-3, quite good refinement in structure has been achieved, even though the spheroids are not regular. In ten cycled sample, cementite spheroids have joined with each other and led to coarse microstructure. However by changing the quenching medium from oil to water, considerable refinement could be achieved. This is because of very fast cooling by which grain boundary precipitation of cementite is avoided and also cementite nuclei did not get time to grow. It is quite obvious that microstructure can not be refined by thermal cycling to the extent of that, which can be obtained by single quench-isorolling process. In case of

high carbon high chromium steels, the carbides are seen in fine form, but there are locations where the carbides have not been dissolved properly.

In the microstructures of quench-isorolled samples, considerable effect of total % reduction is observed. It is clear that as the % reduction is increased, the structure becomes finer and finer. But the samples, quenched from different austenitization temperature and isorolled for same % reduction, have shown the difference in microstructure. It shows that the austenitization temperature should be high enough to dissolve all carbon before it is subjected to quenching. In this case  $880^{\circ}\text{C}$  is the temperature upto which the specimen should be heated before quenching and isorolling.

Fracture surfaces presented show that the specimen has failed in ductile manner. In addition, some cavities are also observed. By comparison of the microstructures of the samples before mechanical testing with that of after mechanical testing, show that considerable coarsening has occurred during deformation. Moreover black regions showing cavities are quite obvious in structure. It is to note that cavitation plays an important role on the total ductility of the specimen. However grain coarsening and cavitation is less in case of single quench-isorolled samples as compared to thermally cycled samples, which show that the cementite spheroids are more stable in quench-isorolled sample as compared to thermally cycled samples.

## 5.2 Stress-Strain Rate Behaviour:

All the curves plotted for stress-strain rate shows sigmoidal nature, which is a typical characteristic of a superplastic material. The material is expected to obey the following relation :

$$\sigma = KE^m$$

Where  $\sigma$  is the flow stress,  $K$  is a material constant,  $E$  is the strain rate and ' $m$ ' is the strain rate sensitivity index.

The tests were carried out at  $700^\circ\text{C}$  ( $973^\circ\text{K}$ ) which also obeys the requirement of superplastic deformation ( $T > 0.5 T_m$ ). At higher temperature contribution to deformation are made through several independent processes such as (i) Dislocation motion (slip) within grains for ' $m$ '=0.1 to 0.3 (ii) Grain boundary sliding for  $m = 0.5$  etc.

In the plot it is clear that the values of flow stress for treated samples are lower than those of the sample in as received condition. It is still lower in the case of single quench-isorolled samples.

## 5.3 Strain Rate Sensitivity Index-Strain Rate Behaviour:

All the curves shown in the previous Chapter for strain rate sensitivity index-strain rate obeys the typical characteristic of superplastic material. The value of ' $m$ ' increases, reaches to peak and then decreases. It is clear that the value of ' $m$ ' is not as high in case of thermally cycled sample as of single quench-isorolled sample.

It can be explained on the basis of microstructure which is obtained after each treatment. By comparing the microstructures of both the samples obtained by thermal cycling and quench-isorolling technique, it is obvious that the dispersion of cementite globules is better and structure is more fine, in case of quench-isorolled samples so the value of 'm' is high.

#### 5.4 % Elongation-Strain Rate Sensitivity Index:

The results show that as the value of 'm' increases, % elongation also increases. From the equation (1.4) the graph can be plotted. Present data are compared with the standard equation in Fig. 5.1. Lower values can be explained on the basis that the elongation is inferior in strip specimen as compared to round one.

#### 5.5 Superplasticity in High Carbon Steel:

It has been observed that good ductilities can be obtained by various thermo-mechanical treatments. Thermal cycling does not improve grain refinement and also the grains are not stable at higher temperature of deformation. However in case of quench-isorolled samples, good % elongations have been obtained and it can be further increased by increasing % reduction in isorolling. Due to the furnance design attached to rolling mill, it was not possible to go beyond 82% reduction. Moreover by increasing the temperature of deformation, it is possible to obtain higher values of 'm', so % elongations.



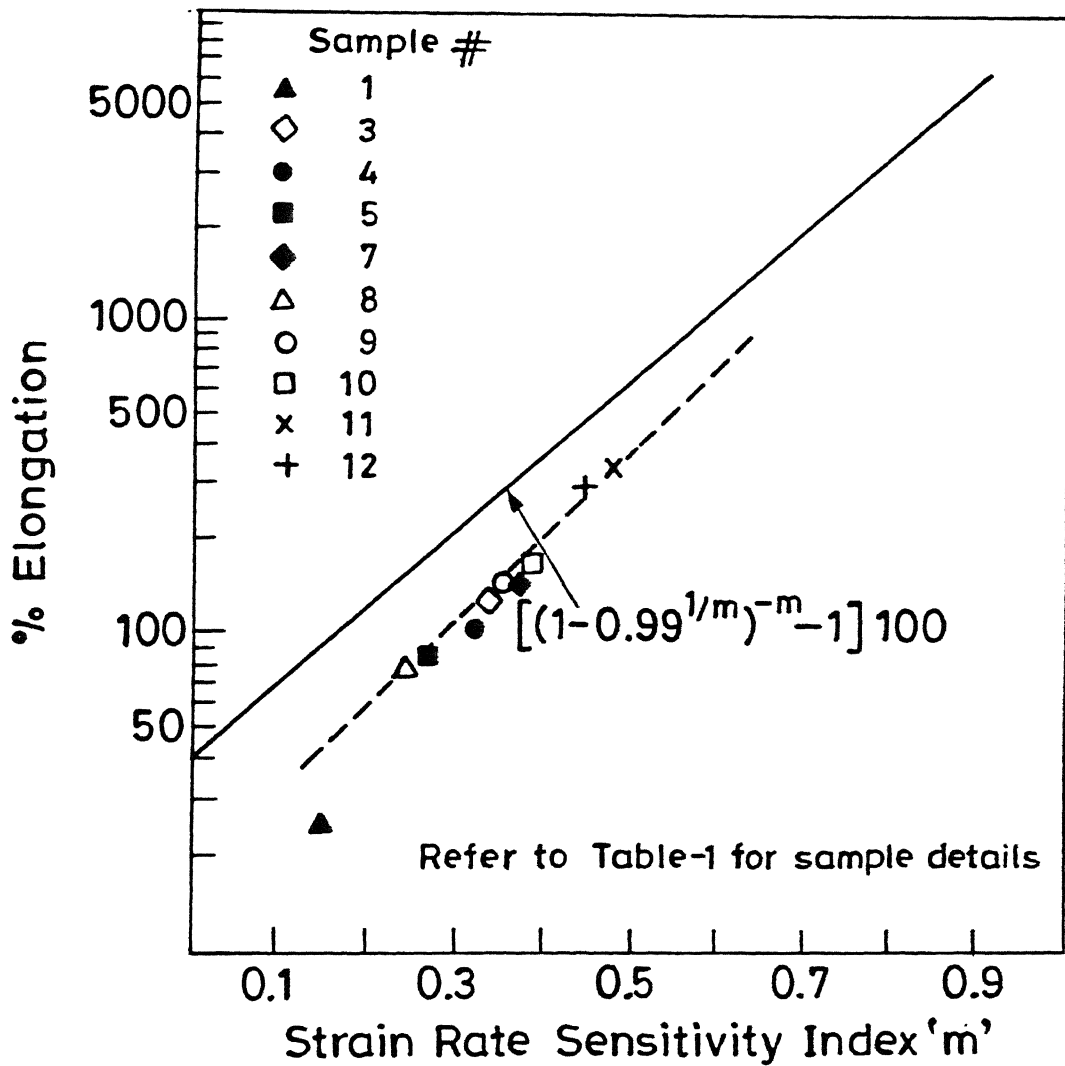


Fig.5.1 Comparison between the standard and present<sup>(2)</sup> relationship between % elongation and 'm'.

In the present study, it has been noted that high carbon steels containing 1.0% carbon should be quenched from 880°C and then isorolled for 79% or more reduction, to get best results of superplasticity.

## CHAPTER VI

### CONCLUSIONS

1. It is possible to heat-treat high carbon steels (1.0% carbon) to get fine structure.
2. Single quench-isorolling technique is better than thermal cycling to obtain uniform, fine and good dispersion of cementite in the structure.
3. Amongst the various thermal cycling processes, quenching in water from  $850^{\circ}\text{C}$  followed by annealing at  $650^{\circ}\text{C}$  for 30 minutes gives the best results of fine structure.
4. In single quench-isorolling techniques; quenching in oil from  $880^{\circ}\text{C}$ , isorolling at  $720^{\circ}\text{C}$  to total % reduction of 79% provides very fine distribution of cementite spheroids in ferrite matrix.
5. As strain rate sensitivity index increases, % elongation also increases.
6. Strain rate sensitivity index depends upon the structure of the phases present. In case of thermal cycling the maximum value of 'm' which can be achieved is 0.38.
7. By single quench-isorolling, strain rate sensitivity index 'm' can be increased to 0.476 and ductilities exceeding 300% can be easily achieved.
8. Grain coarsening during deformation is more in case of thermally cycled steel compared to quench-isorolled steel.

## REFERENCES

1. Dieter, George. E. ''Mechanical Metallurgy'', 2nd edition (1984) 351-353.
2. Morrison, W.B.: Trans. Met. Soc. AIME 242 (1968) 2221.
3. Padmabhan, K.A. ;, Davies, G.J.: ''Superplasticity'', Vol.2 (1980).
4. Chokshi, A.H.; Mukherjee, A.K.: '' The Role of Cavitation in Failure of Superplastic Alloys'', Proceedings ''Superplasticity and Superplastic Forming '' (1988) 149-160.
5. Chokshi, A.H.; Langdon, T.G.: ''A Model for Diffusion Cavity Growth in Superplasticity'', Acta Metall., 35 (1987) 1089-1101.
6. Holt, D.L.; Backofen, W.A.: Trans. Am. Soc. Met. 59 (1966 ) 755.
7. Stewart, M.J.: Metall. Trans. 7A (1976) 399.
8. John, A. Wert.: '' Grain Refinement and Grain Size Control'', Conference Proceedings, ''Superplastic Forming of Structural Alloy'' Edited by N.E. Paton and C.H. Hamilton (1984) 69-83.
9. Peter, S.M. ; Ziegler, G. and Lutjering, G., Z. Metallkunde, 73 (1982).
10. Edington, J.W.: Met. Technol. 3 (1976) 138.
11. Marder, A.R. : Trans. Met. Soc. AIME 245 (1969) 1337.
12. Robbins, J.L.; Shepard, O.C.; Sherby, O.D.: J.I.S.I. 202 (1964) 804.

13. Murthuraj, R.: M.Tech Thesis ''Superplasticity of Ultra-high Carbon Steels'', (1988).
14. Dung, W.K.; Oyama, T.; Sherby, O.D.; Ruano, O.A.; Wodsworth, R.J.: '' Superplastic Ultrahigh Carbon Steels'', Proceedings, ''Superplastic Forming '' ASM (1984) 32-42.

```
C***** INSTRON MECHANICAL TESTING ANALYSIS *****
C***** TENSILE SPECIMEN *****
C
C          0.75inch    0.50inch    0.75inch    0.08inch
C          [-----] [-----] [-----] [----]
C          |         |         |         |
C          +-----+ +-----+ +-----+ +---+
C          0.75inch   0.50inch   0.75inch   0.08inch
C
C***** By R.K.Jindal**
C      V ----- CROSS HEAD VELOCITY **
C      P ----- LOAD **
C      GL(I) --- INSTANTANEOUS GAUGE LENGTH **
C      STRESS -- TRUE STRESS **
C      STNRAT -- TRUE STRAIN RATE **
C      RATE ----ENG. STRAIN RATE **
C      A(I) ----INSTANTANEOUS CROSS SECTIONAL AREA **
C      ENGGST ---ENG. STRESS **
C      DMZ ----- VALUE OF 'm' **
C      AI ----- INITIAL CROSS SECTIONAL AREA **
C      GLI ----- INITIAL GAUGE LENGTH **
C      CHNGL --- TOTAL CHANGE IN GAUGE LENGTH **
C      ITEMP --- TEMPERATURE OF TESTING **
C      IMTN ---- SAMPLE NO. **
C*****
REAL V(50),P(50),GL(50),STRESS(50)
REAL STNRAT(50),SEN(50),RATE(50)
REAL A(50),ENGGST(50),DMZ(50)
REAL AI,GLI,CHNGL
OPEN(UNIT=35,FILE='DATA.IN')
OPEN(UNIT=40,FILE='TEST.OUT')
READ (35,*) N,ITEMP,IMTN
READ (35,*) AI,GLI,CHNGL
READ (35,*)(V(I),P(I),GL(I),I=1,N)
WRITE(40,5) ITEMP
WRITE(40,10) IMTN
WRITE(40,15)
WRITE(40,20)
WRITE(40,30)
5 FORMAT(30X,'MECHANICAL TESTING PERFORMED AT',I4,
1 1X,'DEGREES CENTIGRADE',/)
10 FORMAT(40X,'INSTRON MECHANICAL TESTING ANALYSIS',
1 20X,'FOR SAMPLE -',I2)
15 FORMAT(40X,'*****',20X,
1 '- ',/)
20 FORMAT(1X,'CROSS HEAD',14X,'INSTANT',8X,'INSTANT',8X,'ENG.',4X,
1 'ENGINEERING',6X,'TRUE',8X,'TRUE',7X,'VALUE',5X,)
30 FORMAT(1X,'VELOCITY',5X,'LOAD',4X,'GAUGE LENGTH',7X,
1 'AREA',8X,'STRESS',4X,'STRAIN RATE',5X,'STRESS',3X,'STRAIN RATE',
2 4X,'OF m',4X,/)
DO 100 I=1,N
A(I)=(AI*GLI)/GL(I)
STRESS(I)=P(I)/A(I)
STNRAT(I)=V(I)/(GL(I)*60.0)
RATE(I)=V(I)/(GLI*60.0)
ENGGST(I)=P(I)/AI
ELONG =(CHNGL*100.0)/GLI
IF(I.EQ.1) GO TO 100
DMZ(I)=ALOG(P(I)/P(I-1))/ALOG(V(I)/V(I-1))
100 CONTINUE
DO 245 I=1,N
IF(I.EQ.1) THEN
WRITE(40,44) V(I),P(I),GL(I),A(I),ENGGST(I),RATE(I),
1 STRESS(I),STNRAT(I)
GO TO 245
ENDIF
WRITE(40,45) V(I),P(I),GL(I),A(I),ENGGST(I),RATE(I),
1 STRESS(I),STNRAT(I),DMZ(I)
CONTINUE
245 FORMAT(2X,F5.3,4X,F8.2,5X,F9.3,6X,F6.3,4X,F10.3,3X,E10.2,5X
1 ,F8.3,2X,E10.2//)
45 FORMAT(2X,F5.3,4X,F8.2,5X,F9.3,6X,F6.3,4X,F10.3,3X
1 ,E10.2,5X,F8.3,2X,E10.2,4X,F7.3,/)
WRITE(40,60) ELONG
WRITE(40,65)
60 FORMAT(50X,'PERCENTAGE ELONGATION =',F6.2,'%')
65 FORMAT(50X,'-----')
STOP
END
```

MECHANICAL TESTING PERFORMED AT 700 DEGREES CENTIGRADE

INSTRON MECHANICAL TESTING ANALYSIS  
\*\*\*\*\*

FOR SAMPLE -11  
-----

CROSS HEAD VELOCITY	LOAD	INSTANT GAUGE LENGTH	INSTANT AREA	ENGG. STRESS	ENGINEERING STRAIN RATE	TRUE STRESS	TRUE STRAIN RATE	VALUE OF $\epsilon$
.050	18.00	10.200	8.175	2.184	.82E-04	2.202	.82E-04	
.100	23.00	10.480	7.957	2.791	.16E-03	2.891	.16E-03	.354
.200	32.00	11.600	7.189	3.883	.33E-03	4.451	.29E-03	.476
.500	44.50	12.800	6.515	5.400	.82E-03	6.831	.65E-03	.360
1.000	55.00	12.950	6.439	6.675	.16E-02	8.541	.13E-02	.306
2.000	66.00	13.100	6.366	8.010	.33E-02	10.368	.25E-02	.263

PERCENTAGE ELONGATION =363.44X  
-----

DATA INPUT FOR ANALYSIS OF SAMPLE - 11  
\*\*\*\*\*

6	700	11
8.24	10.12	36.78
0.05	18.0	10.20
0.10	23.0	10.48
0.20	32.0	11.6
0.50	44.5	12.80
1.00	55.0	12.95
2.00	66.0	13.10

112198

## Date Slip

This book is to be returned on the  
date last stamped.

[illegible]

ME-1991-M-JIN-SUP